ATOMINSTITUT

TECHNISCHE UNIVERSITÄT WIEN
Vienna University of Technology

Polycapillary Optics for Advanced X-ray Instrumentations

P. Wobrauschek

wobi@ati.ac.at

Atominstitut,
Vienna University of Technology
AUSTRIA

Prof. Muradin Kumakhov

Prof. Kumakhov was Founder and Director
Of the Institue of Roentgen Optics
150 scientific publications and a lot of Patents

M.A.Kumakhov, Radiation of Channeled Particles(Energoatomizdat,Moscow,1986).

Sad news
Prof. Kumakhov
passed away on June 23,2014

He contributed immensly to Science and to the Channeling Conferences

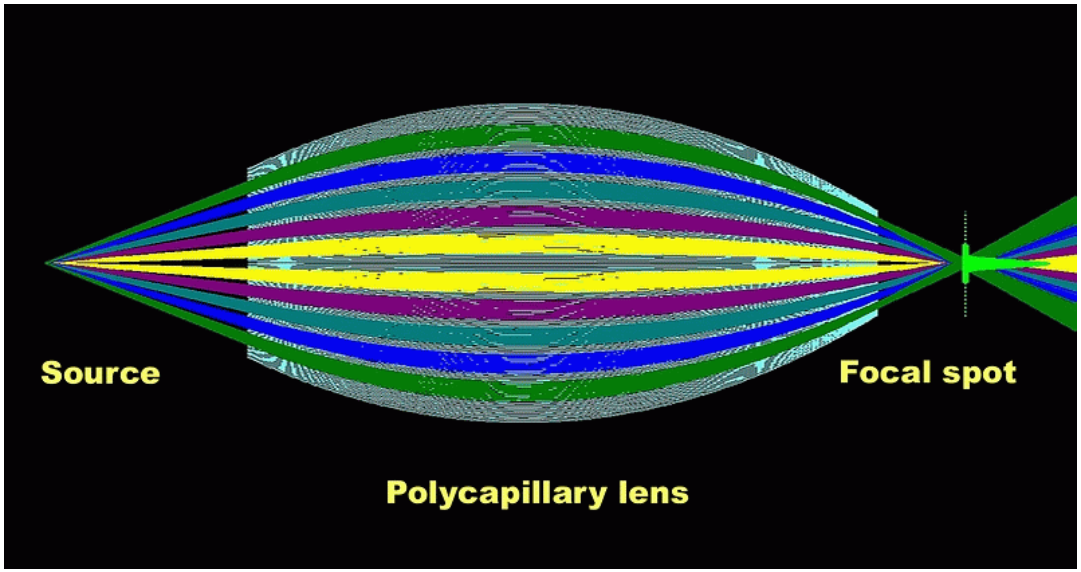

C.W.Röntgen 1895

Discovered X-rays Nov. 8 1895 made
A large number of experiments with the new kind of radiation:
Some conclusions were correct as absorption phenomena and ionizing effects

- X-rays cannot be refracted
- X-rays cannot be reflected
- X-rays propagate straight

Compton

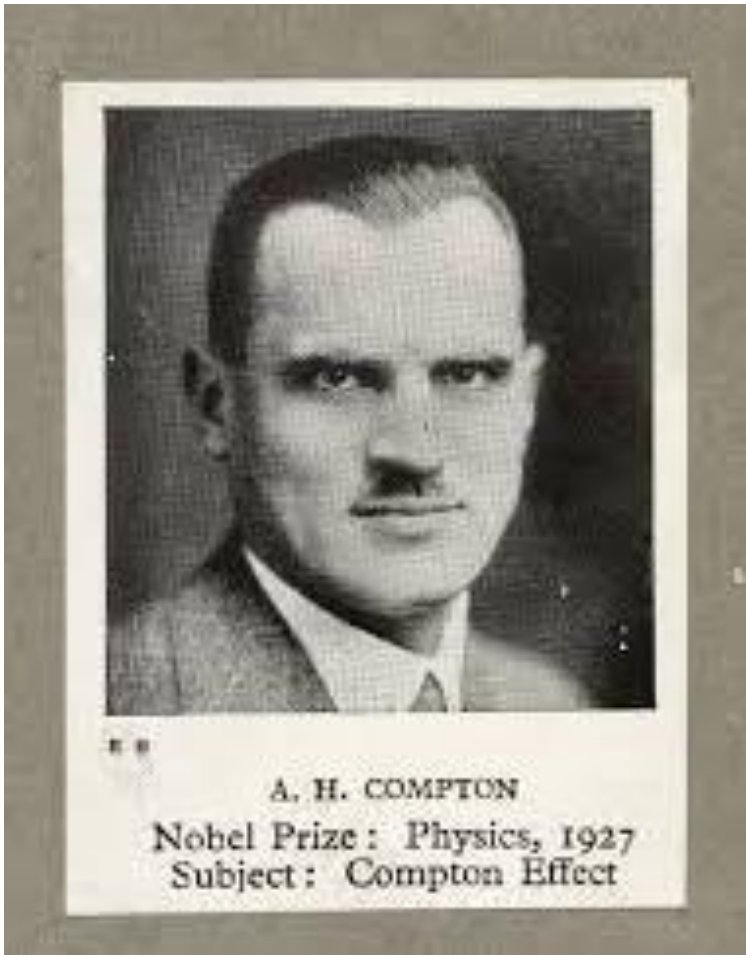

Experimental evidence of Total reflection of X-rays

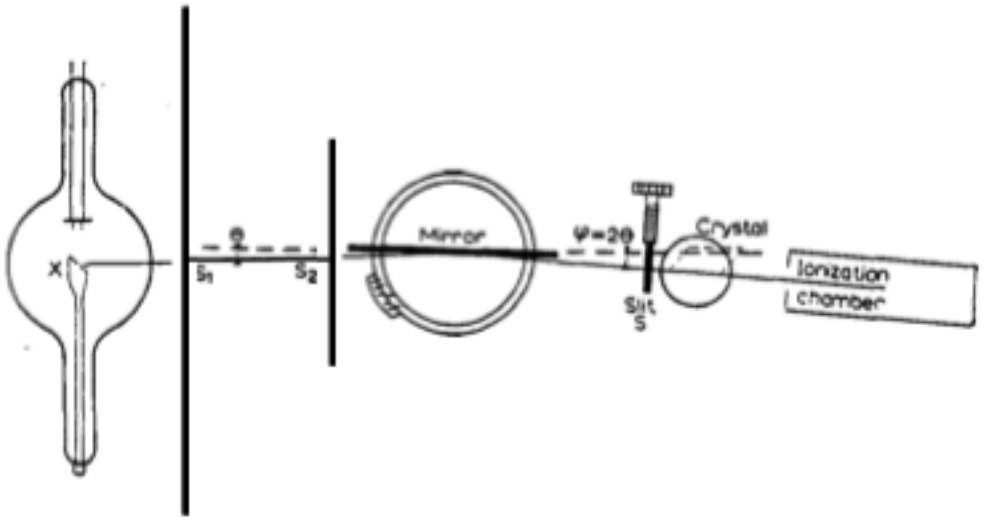

Fig. 1. Apparatus for studying the total reflection of X-rays.

Comptons nobel laureate lecture

The refraction ad reflection of X-rays

We should consider the phenomena of refraction and reflection as one problem, since it is a well-known law of optics that reflection can occur only from a boundary surface between two media of different indices of refraction. If one is found, the other must be present.

In his original examination of the properties of X-rays, Röntgen[1] tried unsuccessfully to obtain refraction by means of prisms of a variety of materials such as ebonite, aluminum, and water. Perhaps the experiment of this type most favorable for detecting refraction was one by Barkla[2]. In this work X-rays of a wavelength which excited strongly the characteristic K-radiation from bromine were passed through a crystal of potassium bromide. The precision of his experiment was such that he was able to conclude that the refractive index for a wavelength of 0.5 Å probably differed from unity by less than five parts in a million.

Refraction observed

Although these direct tests for refraction of X-rays were unsuccessful, Stenström observed[3] that for X-rays whose wavelengths are greater than about 3 Å, reflected from crystals of sugar and gypsum, Bragg's law, $n\lambda = 2D \sin\theta$, does not give accurately the angles of reflection. He interpreted the difference as due to an appreciable refraction of the X-rays as they enter the crystal. Measurements by Duane and Siegbahn and their collaborators[4] showed that discrepancies of the same type occur, though they are very small indeed, when ordinary X-rays are reflected from calcite.

The direction of the deviations in Stenström's experiments indicated that the index of refraction of the crystals employed was less than unity. If this is the case also, for other substances, total reflection should occur when X-rays in air strike a polished surface at a sufficiently sharp glancing angle, just as light in a glass prism is totally reflected from a surface between the glass and air if the light strikes the surface at a sufficiently sharp angle. From a measurement of this critical angle for total reflection it should be possible to determine the index of refraction of the X-rays.

Total external reflection

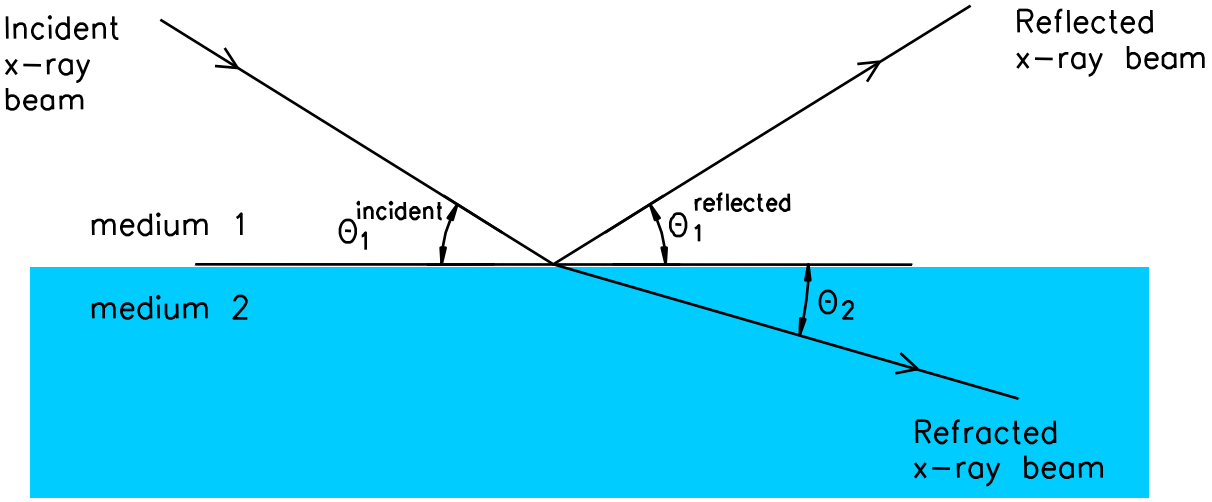

n (x-ray range) $= 1 - \delta - i\beta$

$\delta \sim 10^{-6}$ decrement $\delta \propto f_1(Z)$

$\beta \sim 10^{-8}$ absorption part

φ critical $\approx \sqrt{2\delta} \propto \sqrt{\rho}/E$

$\varphi_{critical}$

(Si, 17.5 keV) $\approx 0.1^\circ$ ≈ 1.75 mrad

(Si, 500 eV) $\approx 3.7^\circ$ ≈ 64.6 mrad

f1 represents the scattering coefficient
thus electronic structure of the atom

PHYSICAL REVIEW VOLUME 95, NUMBER 2 JULY 15, 1954

Surface Studies of Solids by Total Reflection of X-Rays*

L. G. PARRATT
Cornell University, Ithaca, New York
(Received March 22, 1954)

The critical angle and the shape of the observed curve are determined essentially by the electron density and are otherwise independent of the amorphous or crystalline structure, or of the orientation of crystallites on (or in) the surface. If the mirror interface is a sharply defined boundary between two uniform homogeneous media, the dispersion theory predicts the reflection curve. The predicted curve for air and glass is shown

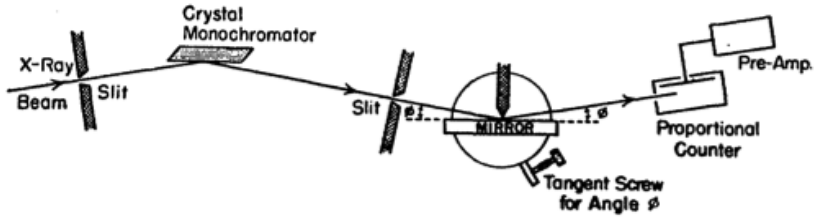

FIG. 1. Experimental arrangement for the x-ray total reflection method of studying smooth solid surfaces.

* This research was supported by the United States Air Force through the Office of Scientific Research of the Air Research and Development Command.

of surfaces) improved experimental techniques in the production and control of the surfaces.

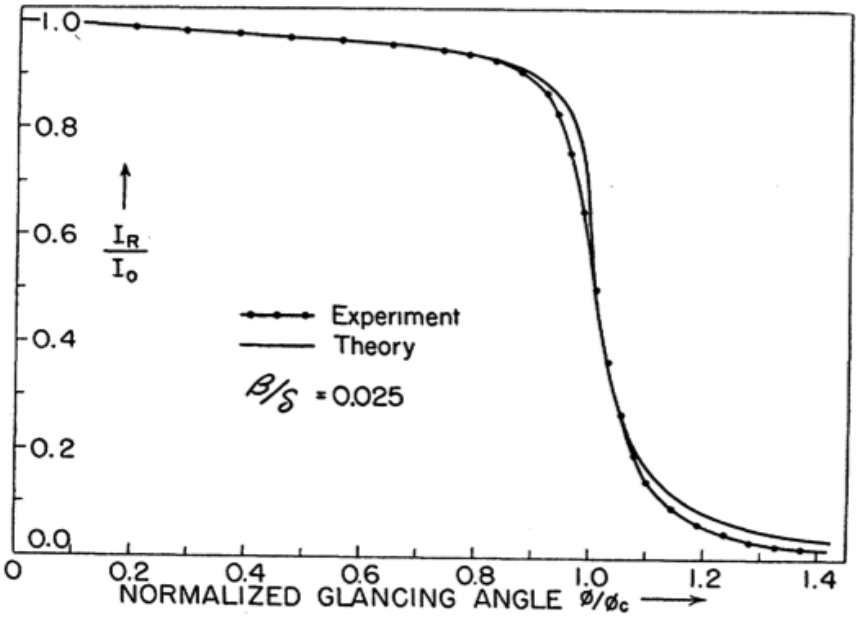

FIG. 2. Intensity reflected from polished glass at small angles of incidence. The angle ϕ_c is the critical angle for total reflection.

Parrat 1954

II. DISPERSION THEORY

Two Homogeneous Media

For any glancing angle, the expressions for the electric vector of the incident beam $E_1(z_1)$, of the reflected beam $E_1^R(z_1)$, and of the refracted beam $E_2(z_2)$ at a perpendicular distance z from the surface, are

$$\left.\begin{aligned} E_1(z_1) &= E_1(0)\exp\{i[\omega t-(k_{1,x}x_1+k_{1,z}z_1)]\} \\ E_1^R(z_1) &= E_1^R(0)\exp\{i[\omega t-(k_{1,x}x_1-k_{1,z}z_1)]\} \\ E_2(z_2) &= E_2(0)\exp\{i[\omega t-(k_{2,x}x_2+k_{2,z}z_2)]\} \end{aligned}\right\}, \quad (1)$$

where k_1 and k_2 are the propagation vectors (of magnitudes $2\pi/\lambda_1$ and $2\pi/\lambda_2$) outside and inside the mirror, respectively, z is taken as positive into the mirror, x, z is the plane of incidence, refraction, and reflection of the beam, and the athwart direction y is parallel to the mirror surface. For x-rays, the glancing angle ϕ_1 (written hereafter without the subscript) is always very small, and we write

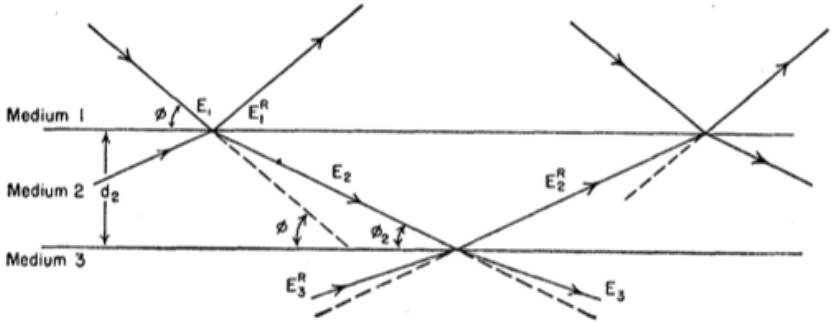

FIG. 4. Sketch of reflection and refraction for stratified homogeneous media.

Shape of the Reflection Curve: Two Media

The Fresnel[1] coefficient for reflection, $F_{1,2}$, can be written

$$F_{1,2}=\frac{E_1^R}{E_1}=\frac{\sin\phi-r_2\sin\phi_2}{\sin\phi+r_2\sin\phi_2}\doteq\frac{\phi-f_2}{\phi+f_2}=\frac{f_1-f_2}{f_1+f_2}, \quad (3)$$

where

$$f_1=(\phi^2-2\delta_1-2i\beta_1)^{\frac{1}{2}}=\phi.$$

X-ray Mirrors and X-ray reflection

The interaction of X-rays with atomic electrons in a substance is described by the complex dielectric constant: $\varepsilon = 1 - 2\delta - 2i\beta$ which yields the complex index of refraction:

$$n = \sqrt{\varepsilon} = 1 - \delta - i\beta$$

The small quantities δ and β are related to dispersive and absorptive natures of the material and given at X-ray wavelengths far from the absorption edges by:

$$\delta = n e^2 \lambda^2 / 2\pi mc^2 \qquad \beta = \mu\lambda / 4\pi$$

n ...total number of dispersive electrons per unit volume of the material
μ ...linear absoprtion coefficient.
As the refractive index is less than unity, X-rays incident on a material are totally reflected if the glancing angle Θ is less than the critical angle Θ_C:

$$\Theta_c = \sqrt{2\delta} = 28.8 \times \frac{1}{E} \times \sqrt{\frac{Zr}{A}}$$

reflec tivity curves for uncoated and gold coated quartz mirrors for 1.5 Å (8.04 keV).

➔**heavy metals,** deposited on the mirror surface, **degrade the sharpness** of the **cut-off** as well as the **reflectivity near the critical angle**.

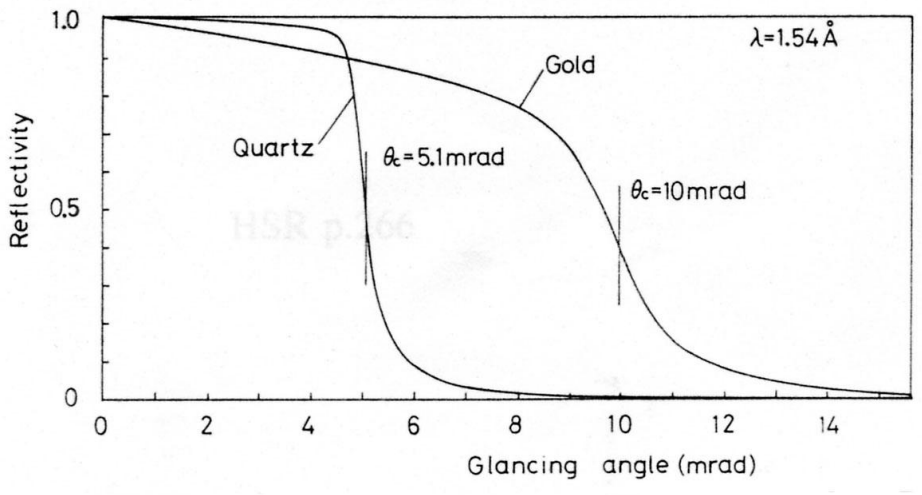

As Θ_c is proportional to λ, a mirror set at a glancing angle Θ does not reflect wavelength shorter than

$$\lambda_c = \Theta\sqrt{\frac{\pi mc^2}{ne^2}} \qquad E_c(\text{keV}) = \frac{32.2}{\Theta_c^{Si}(\text{mrad})}$$

present in the incident beam.

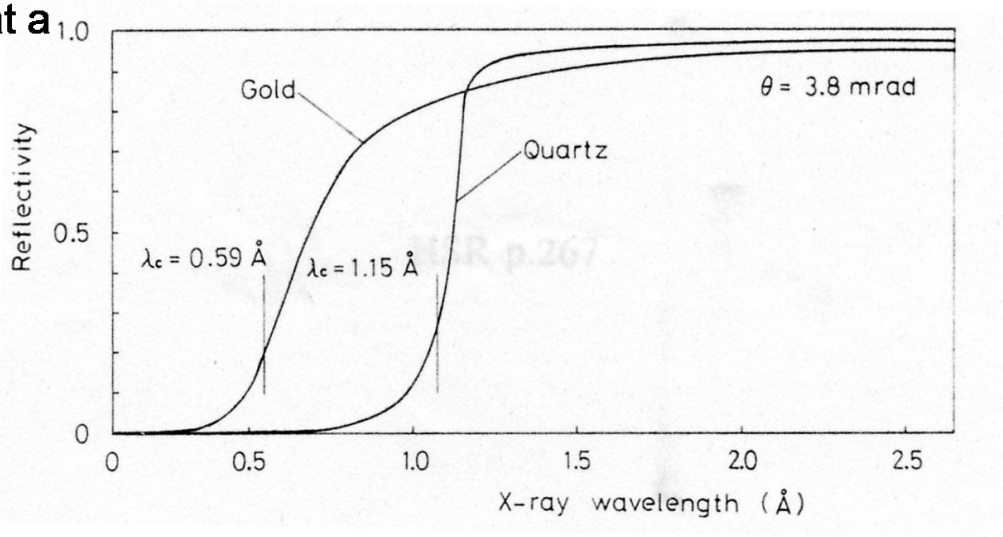

Total reflection effect

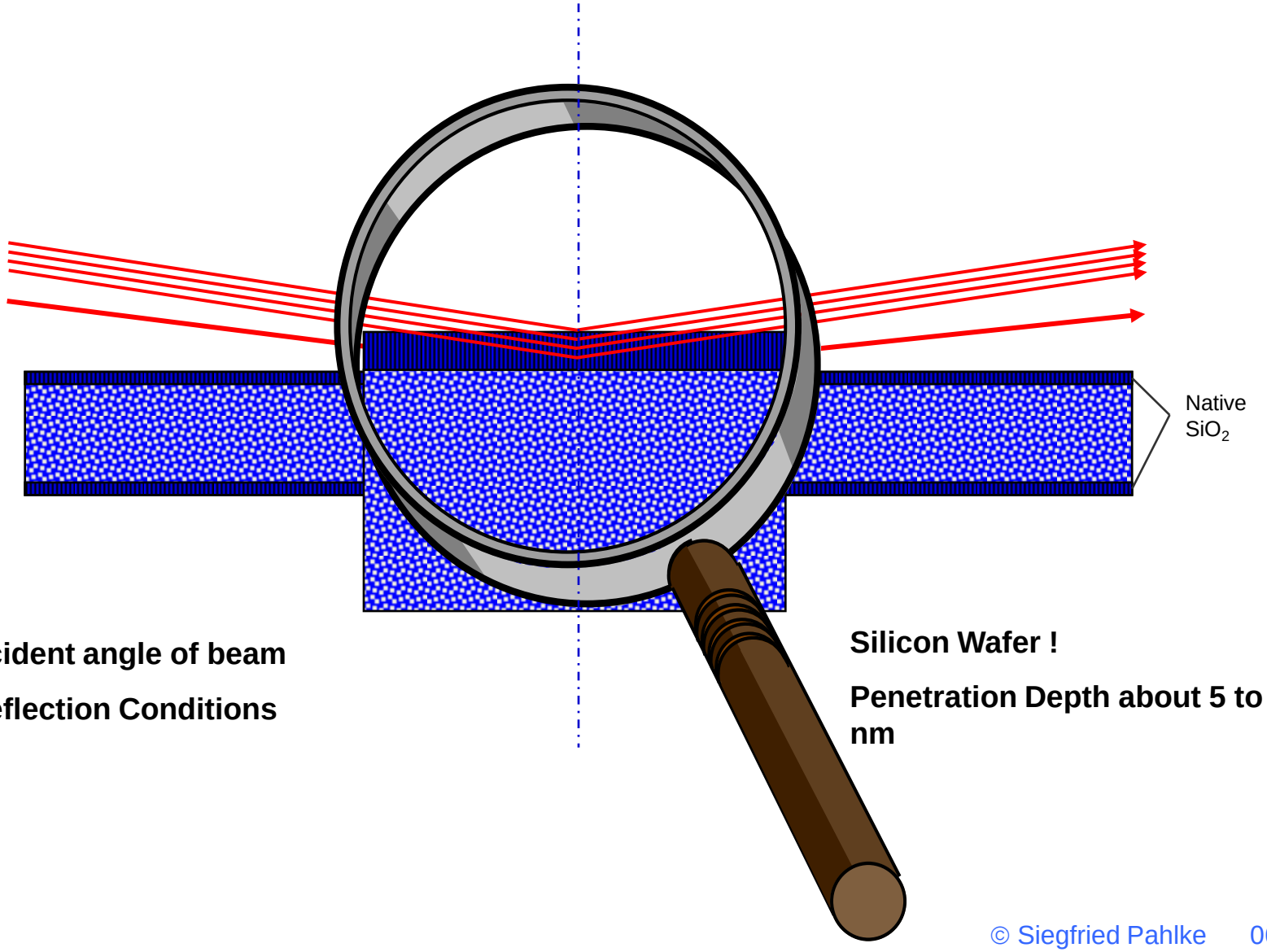

1 mrad incident angle of beam

In Total Reflection Conditions

Silicon Wafer !

Penetration Depth about 5 to 10 nm

Monocapillaries

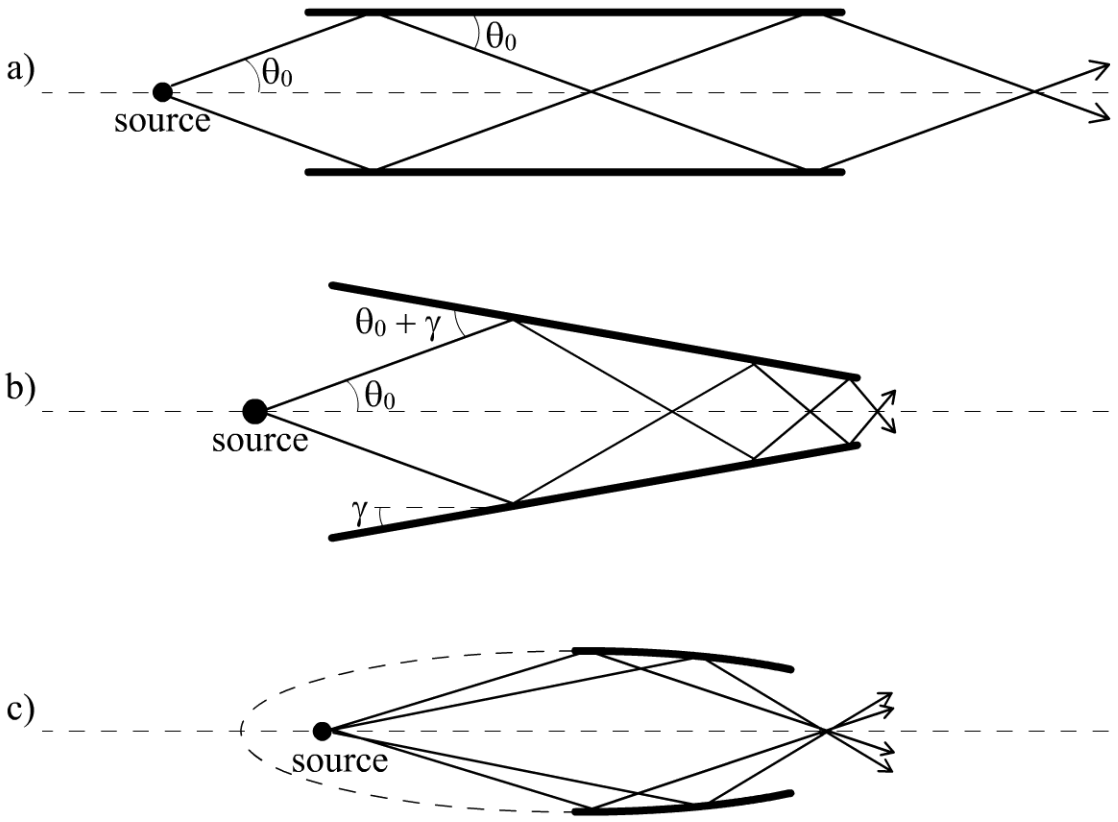

Glass capillary optics

Christian Riekel
ESRF

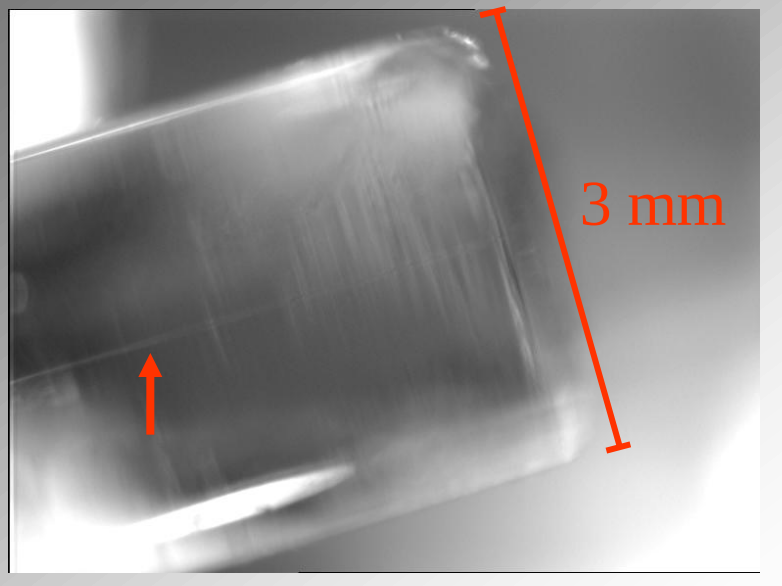

tapered borosilicate capillary

length about 100 mm

2 μm diameter full width at base

2.3 mrad divergence @ 13 keV

flux	$\leq 3*10^{10}$	ph/s/100mA
flux density	$\leq 1*10^{10}$	ph/s/μm^2/100mA

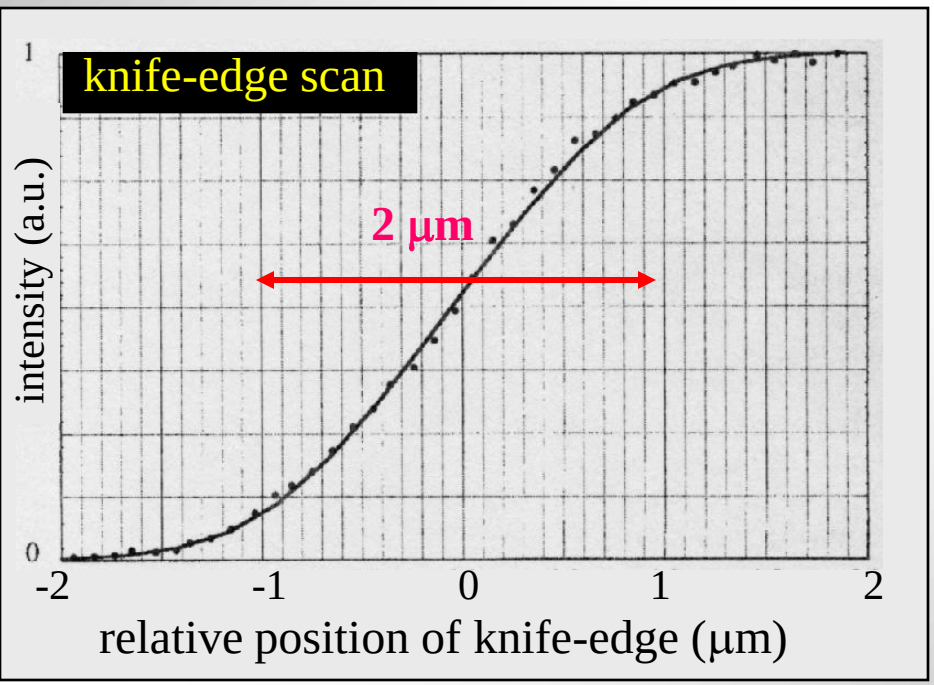

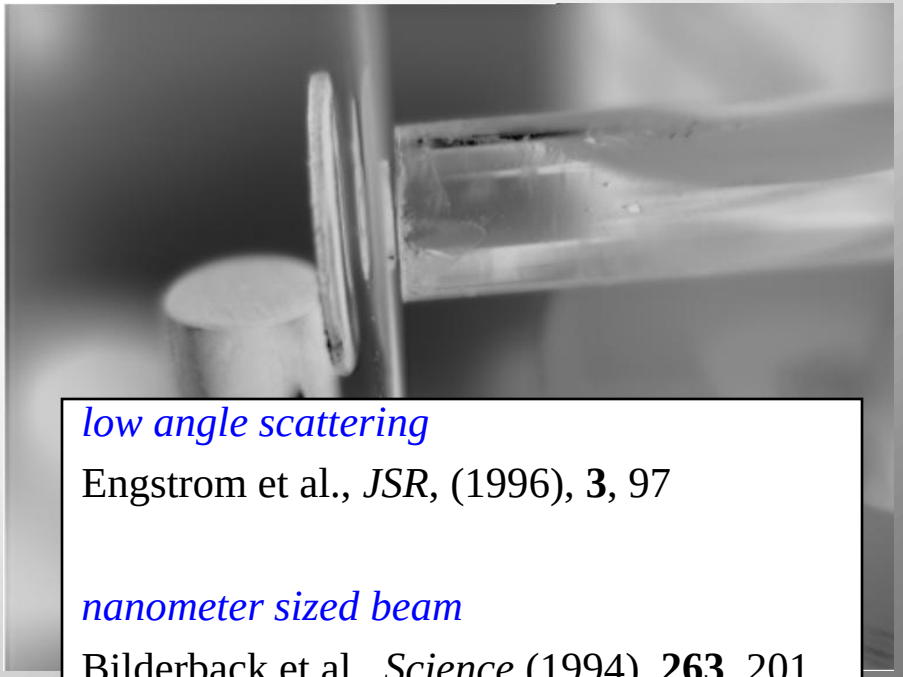

low angle scattering

Engstrom et al., *JSR*, (1996), **3**, 97

nanometer sized beam

Bilderback et al., *Science* (1994), **263**, 201

X-ray Optics 2

Polycapillaries

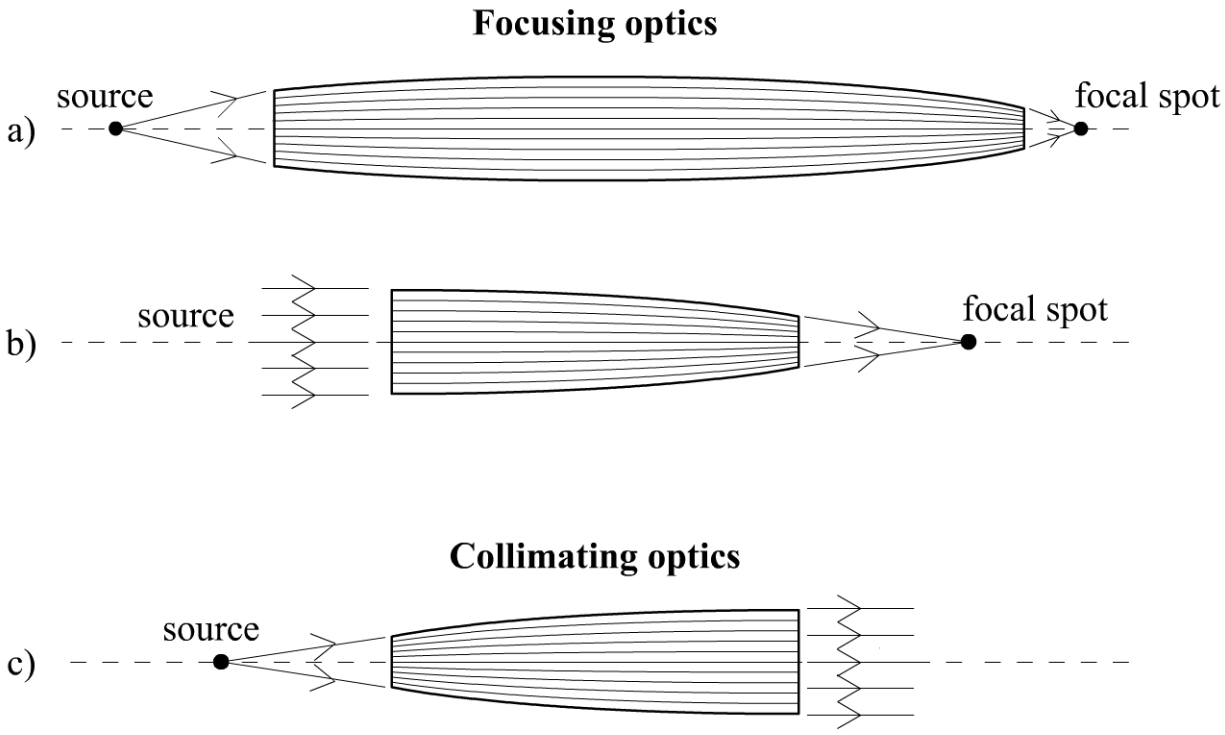

Polycapillary (Kumakhov lense)

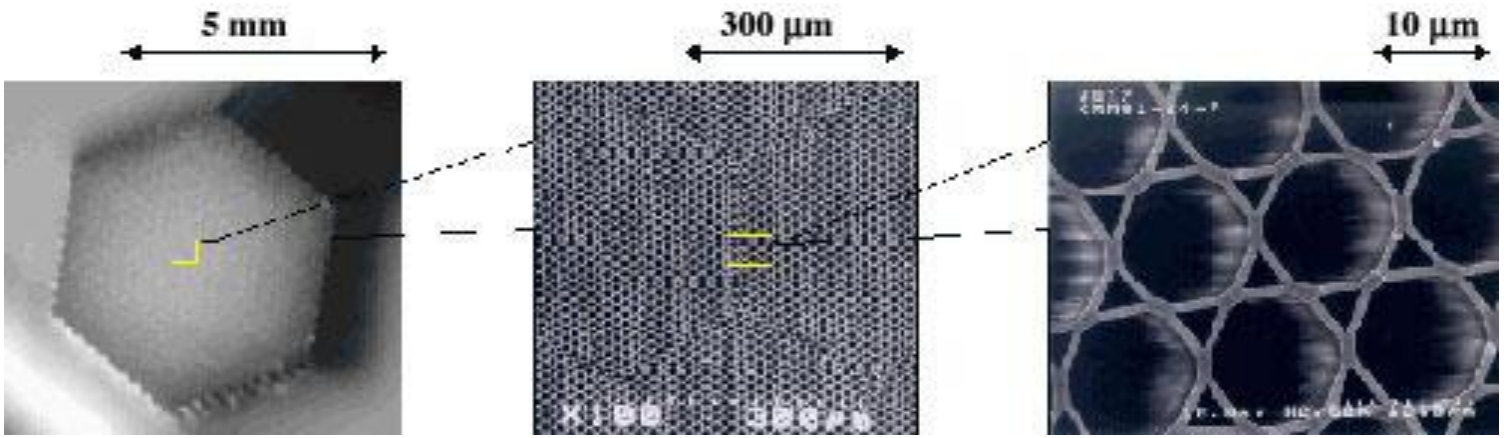

Capillary X-ray optics use hollow capillaries for controlling incident X-rays in many, varied X-ray applications. These optics are formed from a single capillary (monocapillary), or up to several million hollow glass capillaries (polycapillary) that have been fused together and tapered to desired profiles. The principle behind their operation is multiple total external reflection of X-rays along the smooth inner walls of the capillary channels. Reflection of X-ray photons occurs at the boundary between media with different refractive indices. When an X-ray strikes the reflecting surface of a capillary at a grazing angle smaller than the critical angle of the material, it undergoes total external reflection. X-rays satisfying the total reflection condition can be effectively transported through the capillary channels, and therefore formed into a desired wavefront pattern defined by the shaped profile of the optic.

Principle of EDXRS

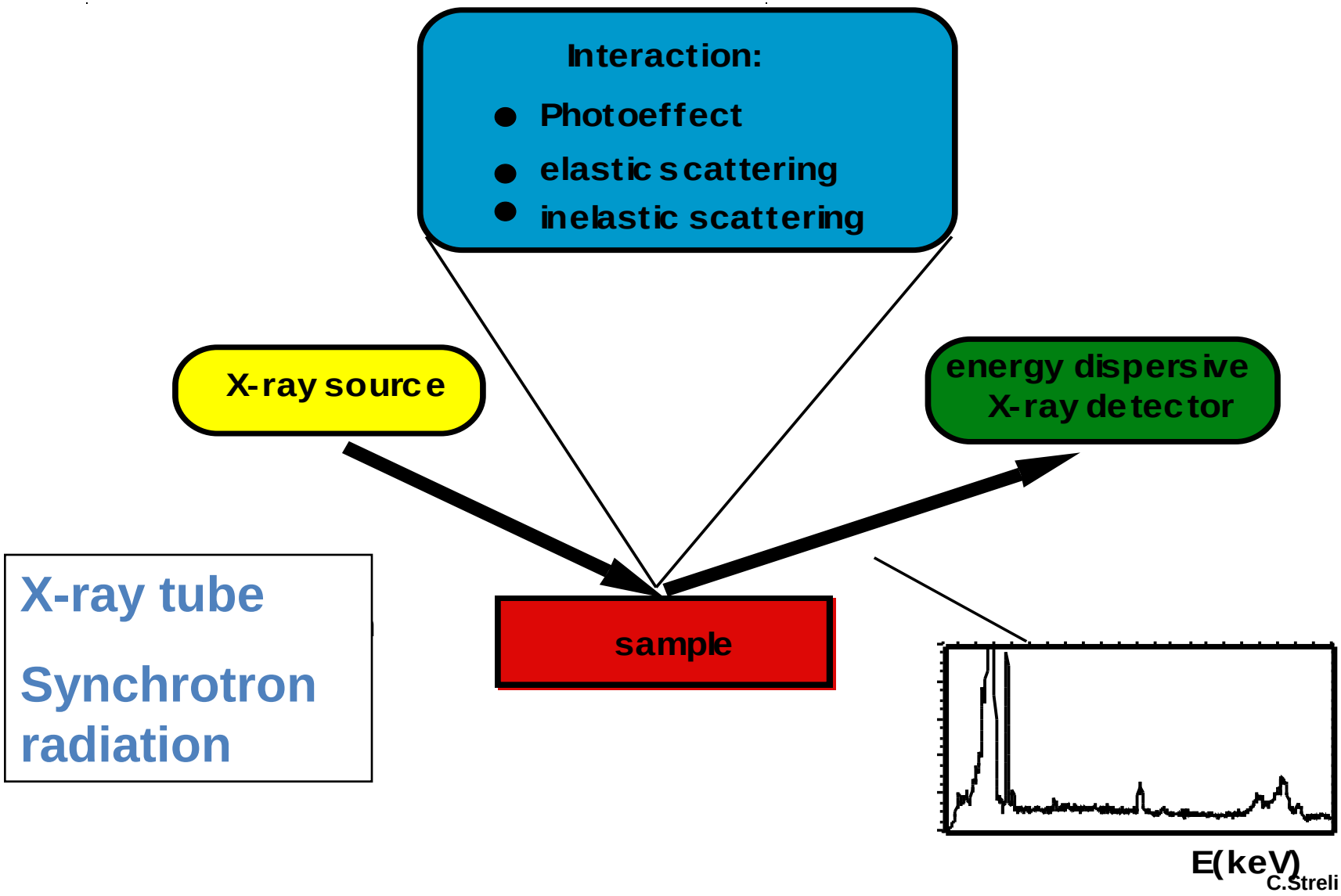

X-ray tube

Synchrotron radiation

Multielement spectrum

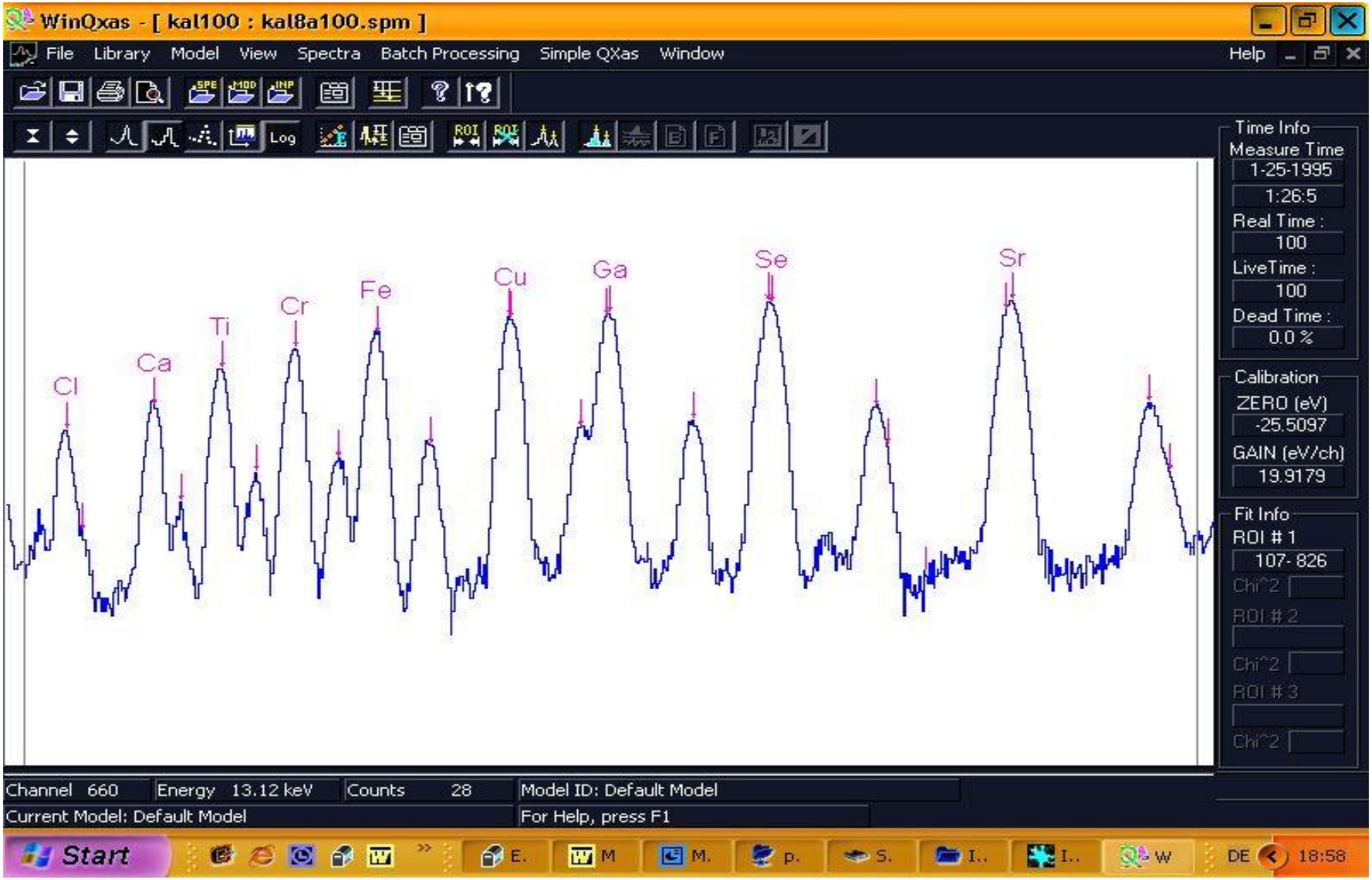

Multielement spectrum evaluted

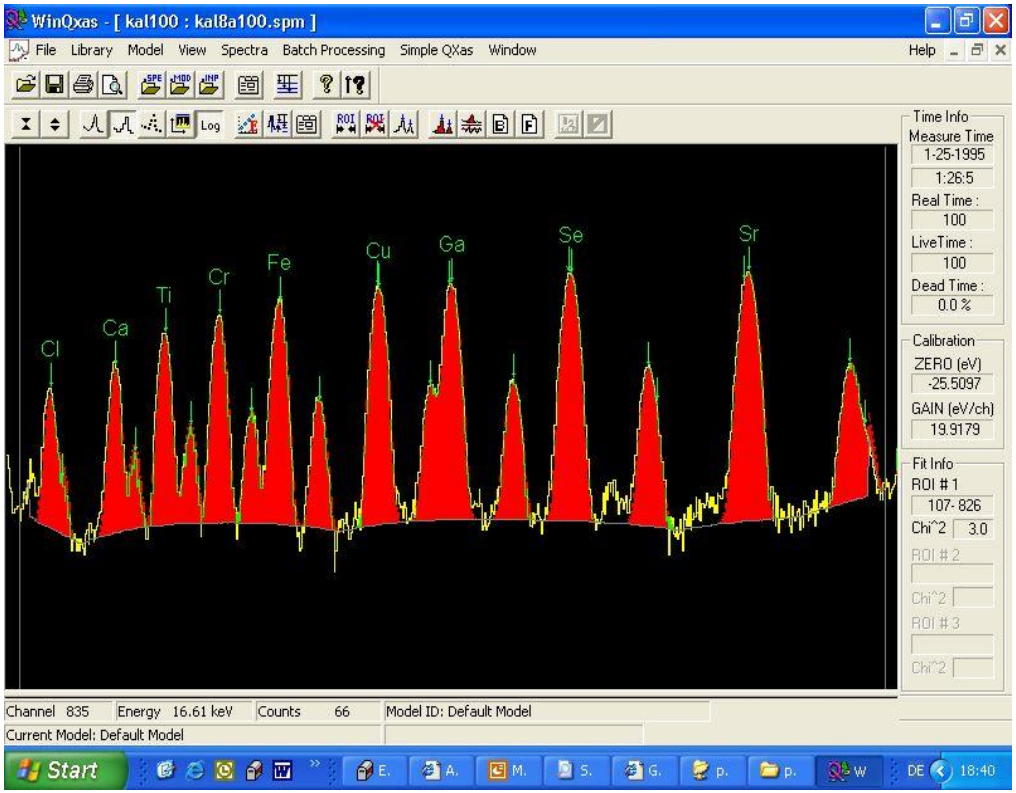

WinQXAS version 1.30, Aug.2001 Feb, 19 2003 06:46:45

Document filename: kal100
Spectrum ID: kal8a100.spm
Model ID: Default Model

Fitting Region: channels 107 - 826, Chisquare = 3.0

Line	E(KeV)	Peak area	st. dev	Chi-sq
Cl - KA1	2.622	2741	± 55	3.8
Cl - KB1	2.816	582	± 21	7.2
Ca - KA1	3.691	4934	± 71	3.5
Ca - KB1	4.013	935	± 23	12.3
Ti - KA1	4.509	10079	± 99	2.0
Ti - KB1	4.932	1662	± 26	8.5
Cr - KA1	5.412	15181	± 121	2.1
Cr - KB1	5.947	2254	± 28	3.0
Fe - KA1	6.399	21380	± 141	2.1
Fe - KB1	7.059	3140	± 29	2.0
Cu - KA1	8.048	19514	± 111	1.6
Cu - KA2	8.028	10005	± 60	1.5
Cu - KB1	8.905	4137	± 33	0.9
Ga - KA1	9.252	21789	± 117	2.2
Ga - KA2	9.225	11201	± 64	2.1
Ga - KB1	10.263	4769	± 34	0.7
Se - KA1	11.222	28584	± 131	1.7
Se - KA2	11.181	14733	± 71	1.6
Se - KB1	12.494	6574	± 38	0.8
Se - KB2	12.652	361	± 23	1.6
Sr - KA1	14.165	31734	± 138	1.3
Sr - KA2	14.098	16510	± 75	1.3
Sr - KB1	15.832	7690	± 44	0.9
Sr - KB2	16.085	986	± 38	14.4

Intensity of fluorescence radiation

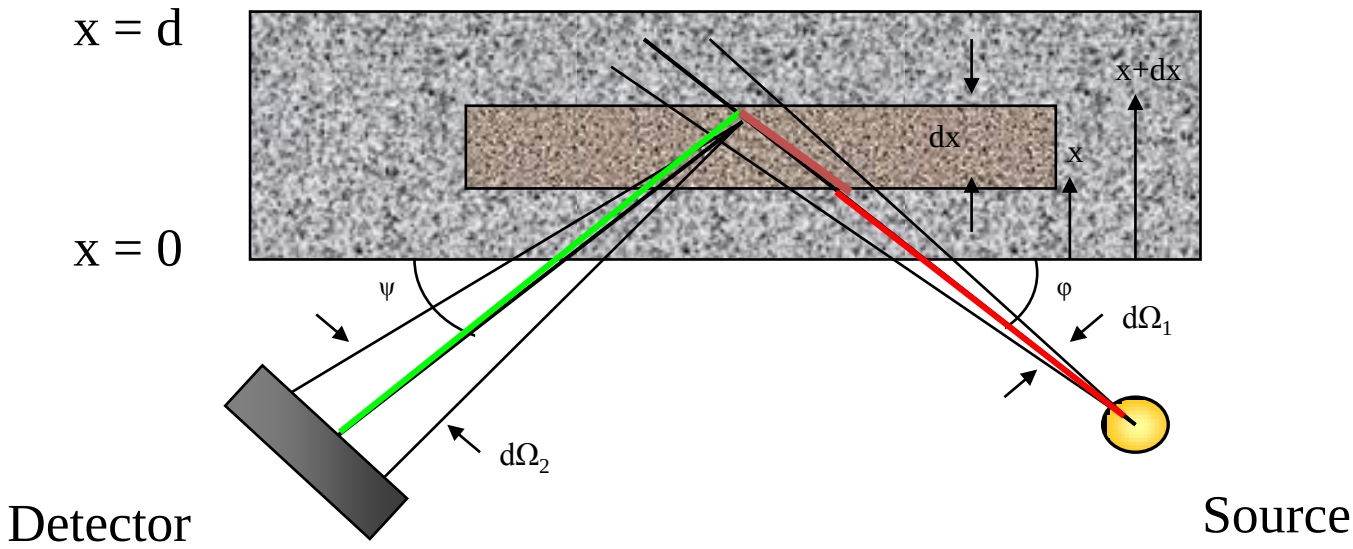

$$I(E^i_{K\alpha}) = \int_{E=E^i_{abs}}^{E=E_{max}} \int_{x=0}^{x=d} I_0(E) \cdot G_1 \cdot \frac{\rho}{\sin\varphi} \cdot \frac{\tau^i_K(E)}{\rho} \cdot \omega^i_K \cdot p^i_\alpha \cdot c^i \cdot V^i(E) \cdot e^{-\left(\frac{\mu(E)}{\rho\cdot\sin\varphi} + \frac{\mu(E^i_{K\alpha})}{\rho\cdot\sin\psi}\right)\cdot\rho\cdot x} \cdot G_2 \cdot f(E^i_{K\alpha}) \cdot \varepsilon(E^i_{K\alpha}) \cdot dx \cdot dE$$

Problems in quantification using polycapillaries

Gain in intensity in focus

Change of energy distribution by high energy cut off

High energy photons pass through central channels

Radial energy distribution due to changes according angle and energy relation

Requirements for light element XRS

- LIGHT ELEMENTS Be B C N O F Ne Na Mg Al Si
- Extreme challenge for EDXRS

- Experiments must be performed in vacuum
- Excitation source with energies close to light element absorption edges and high intensities requested
- Detector window Ultra thin polymer to have efficiency in the low energy region
- Low fluorescence yield

ATI µXRF Spectrometer components

- 50kV/1mA/50W X-ray tube Oxford „Apogee“
  - Mo Anode on HV
  - Cathode grounded
  - Microfocus (35 µm)
  - Thin exit window (125 µm-> Mo-L, 2,3 keV)
  - Air cooled

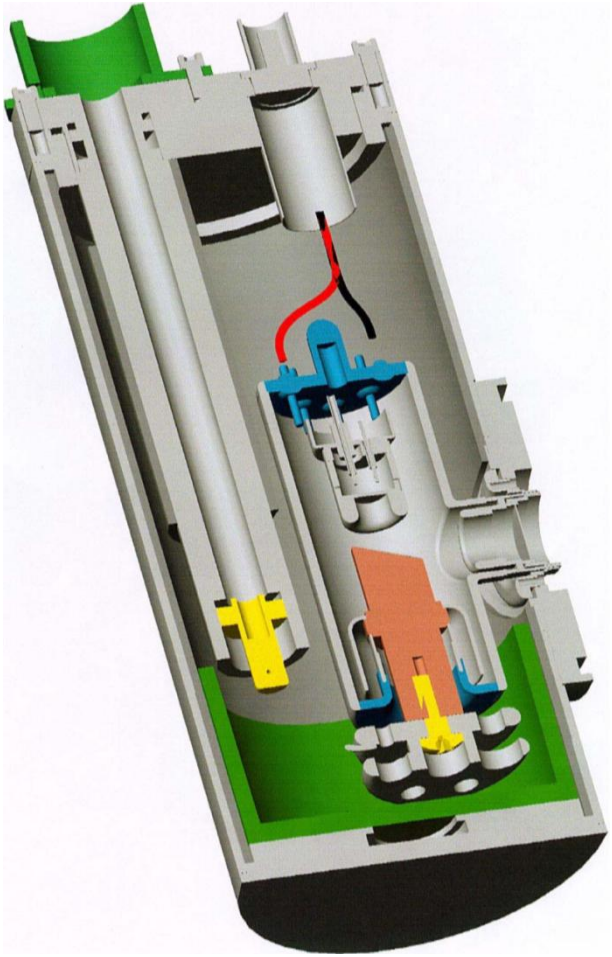

ATI µXRF Spectrometer components

- Polycapillary X-ray optics produced (XOS)
  - Spotsize 32µm @ Mo-Kα (17,44 keV)
  - Intensity gain 39-times (compared to pinhole of 50 µm)
  - 5-Axis adjustable

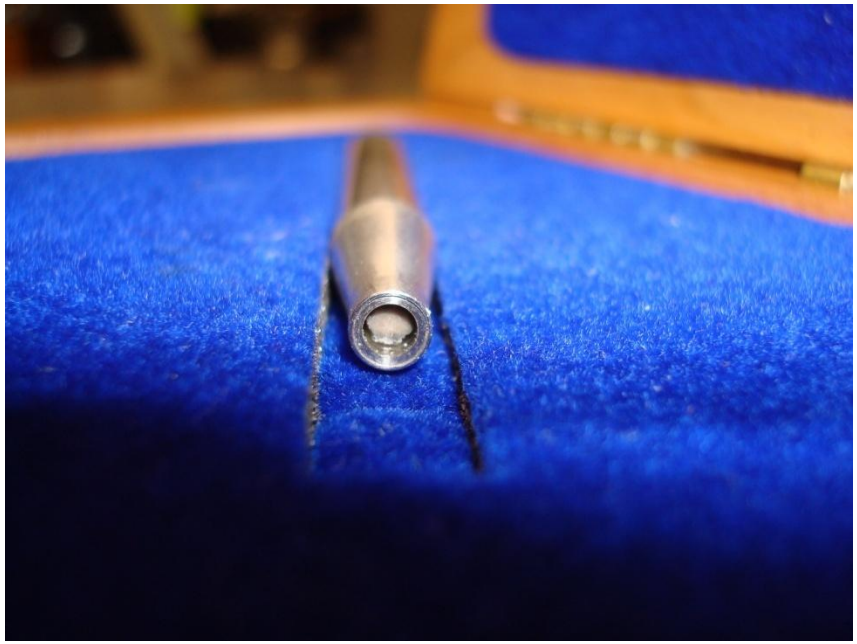

ATI µXRF Spectrometer Design

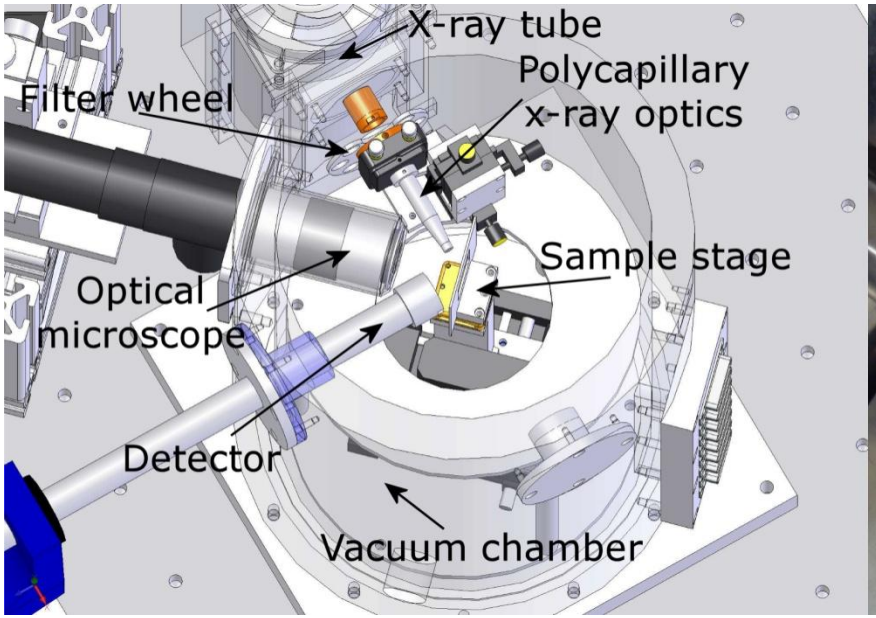

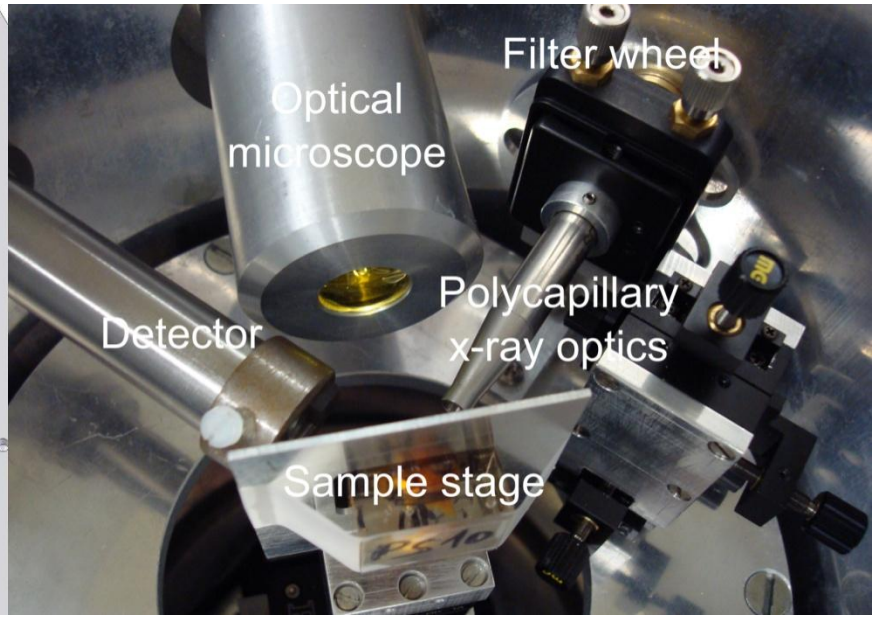

Energy dependence of beam size in focus

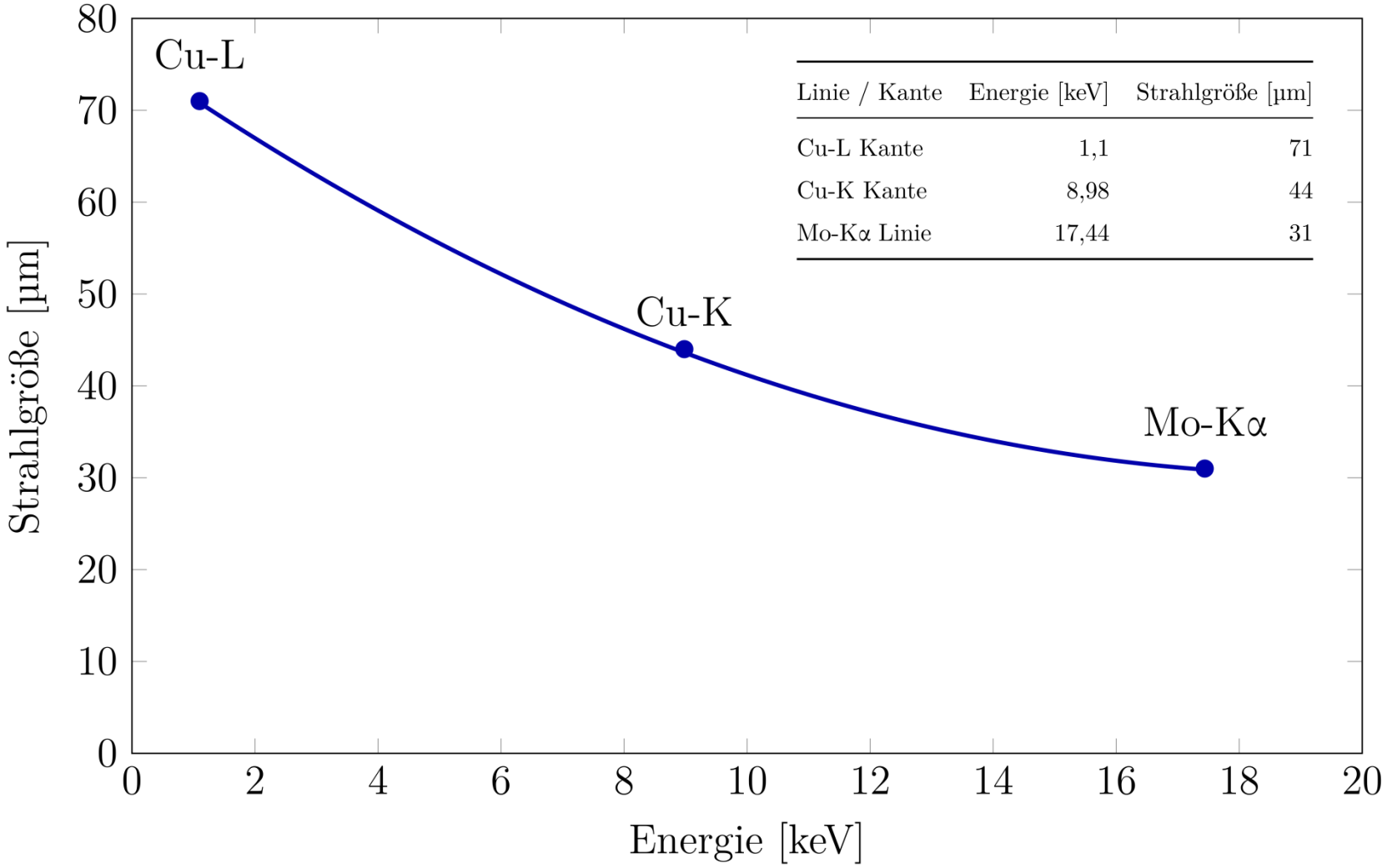

Linie / Kante	Energie [keV]	Strahlgröße [µm]
Cu-L Kante	1,1	71
Cu-K Kante	8,98	44
Mo-Kα Linie	17,44	31

ATI µXRF Spectrometer Resolution

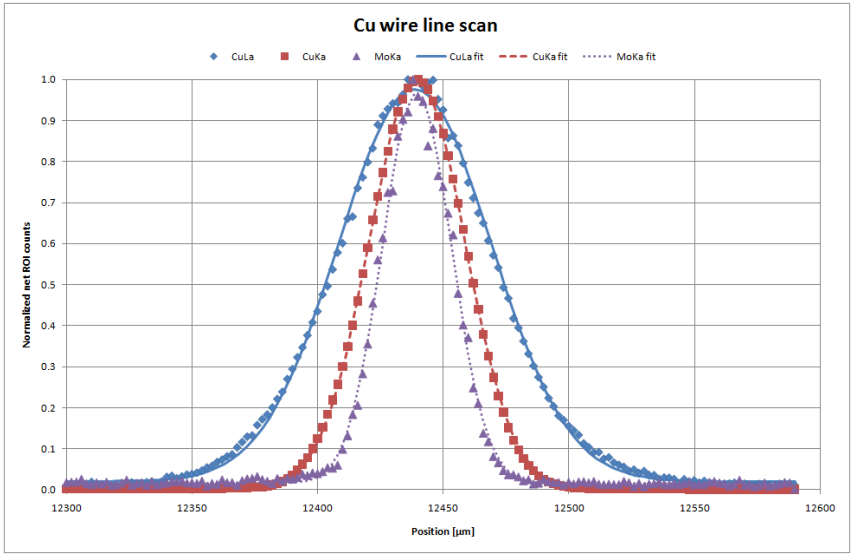

$$FWHM_{beam} \approx \sqrt{FWHM_{profile}^2 - d_{wire}^2}$$

- Determination of minimum beam diameter with a 10µm Cu wire:
  - @ Mo-Kα (17,44 keV): 31 µm
  - @ Cu-K (8,98 keV): 44 µm effektiv
  - @ Cu-L (1,1 keV): 71 µm effektiv

ATI µXRF Spectrometer Software

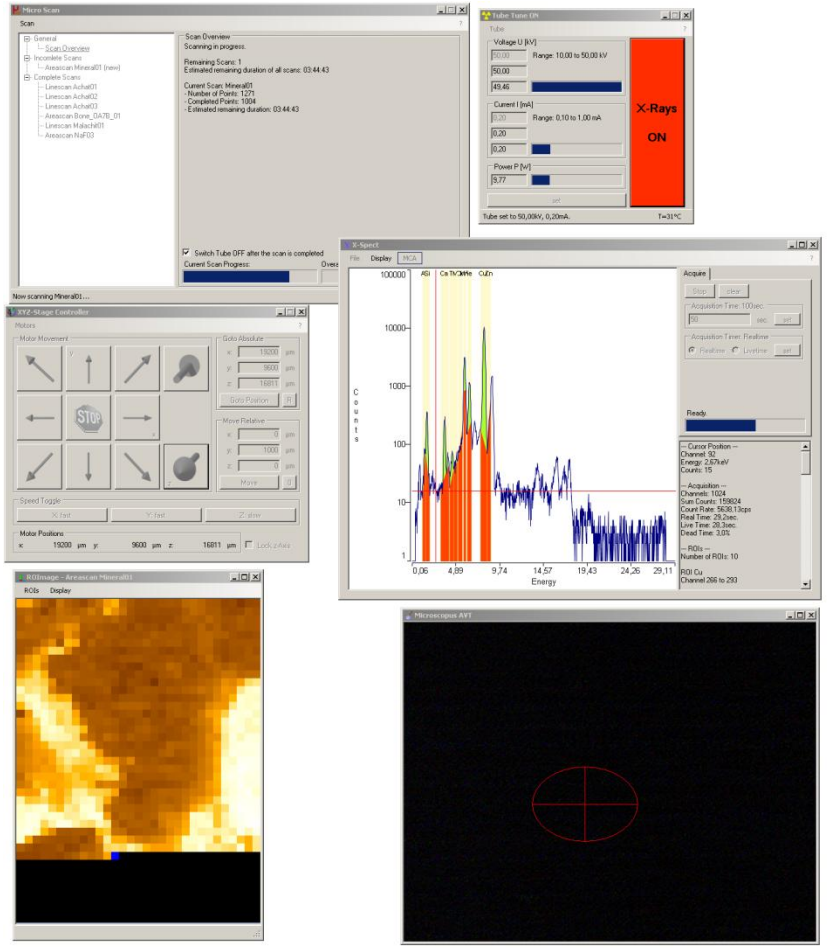

- Software for automatic Mapping of a sample
- Automatic Region of Interest (ROI) Spectrum evaluation with live-preview
- All Spectra stored for later evaluation with software packages as(AXIL,…)

Micro-XRF (µXRF)

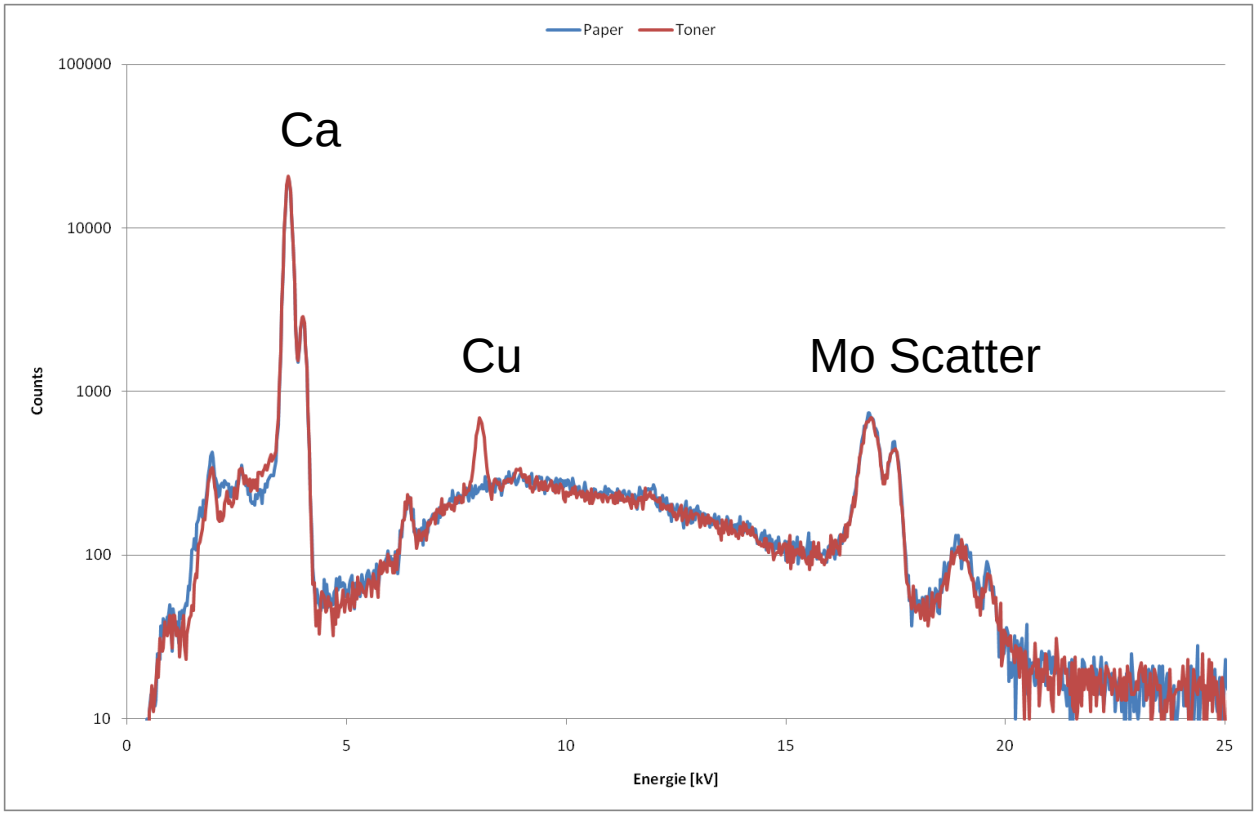

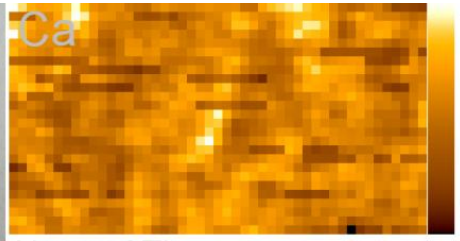

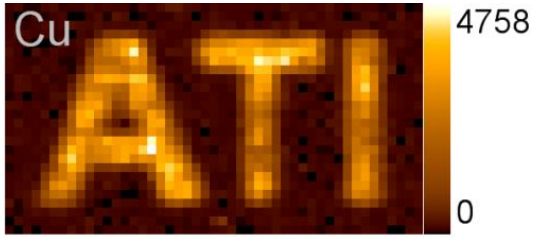

Name: ATI
Scan size: 47x26 pixel
Resolution: 40µm per pixel.
Counting time: 150sec. per pixel
Tube parameters: 50kV, 1mA

ATI µXRF Spectrometer low-Z

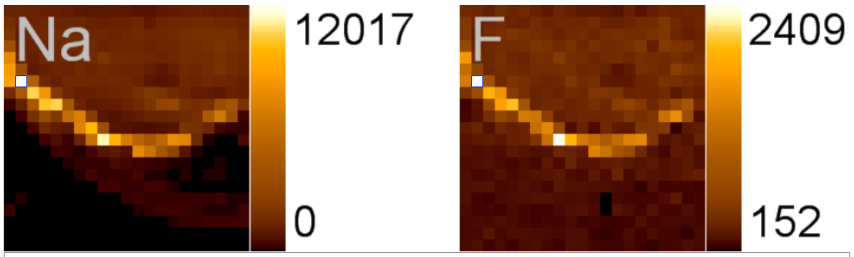

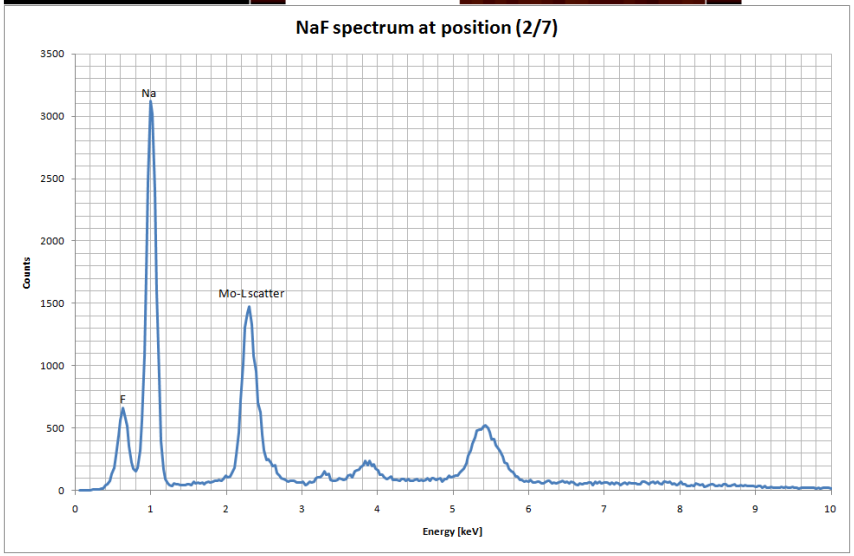

- Analysis of elements with low Z :
  - Mo-L excitation
  - Vacuum
  - UTW Detektor

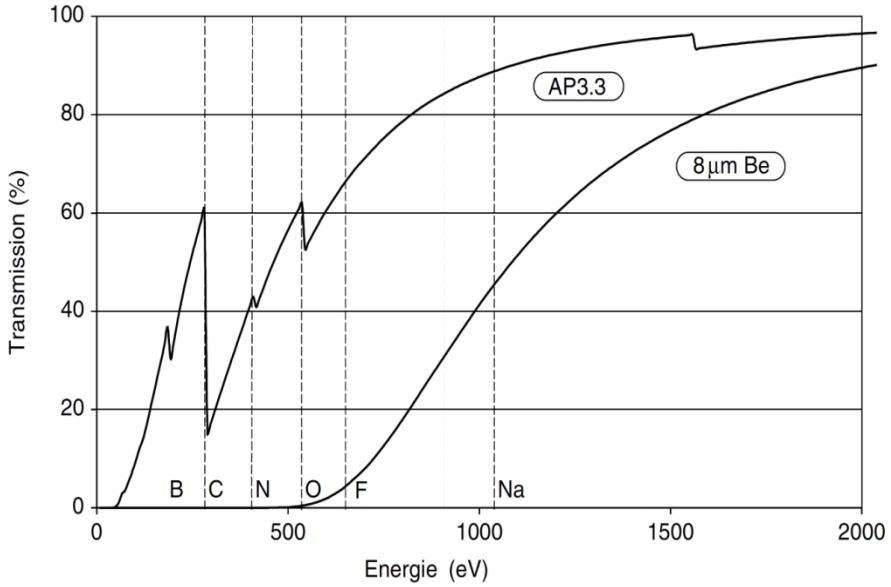

Spectra of NIST 621glass ref. material

- 50 kV / 1 mA
- 10x10 Punkte, je 10 s LT → 1000 s

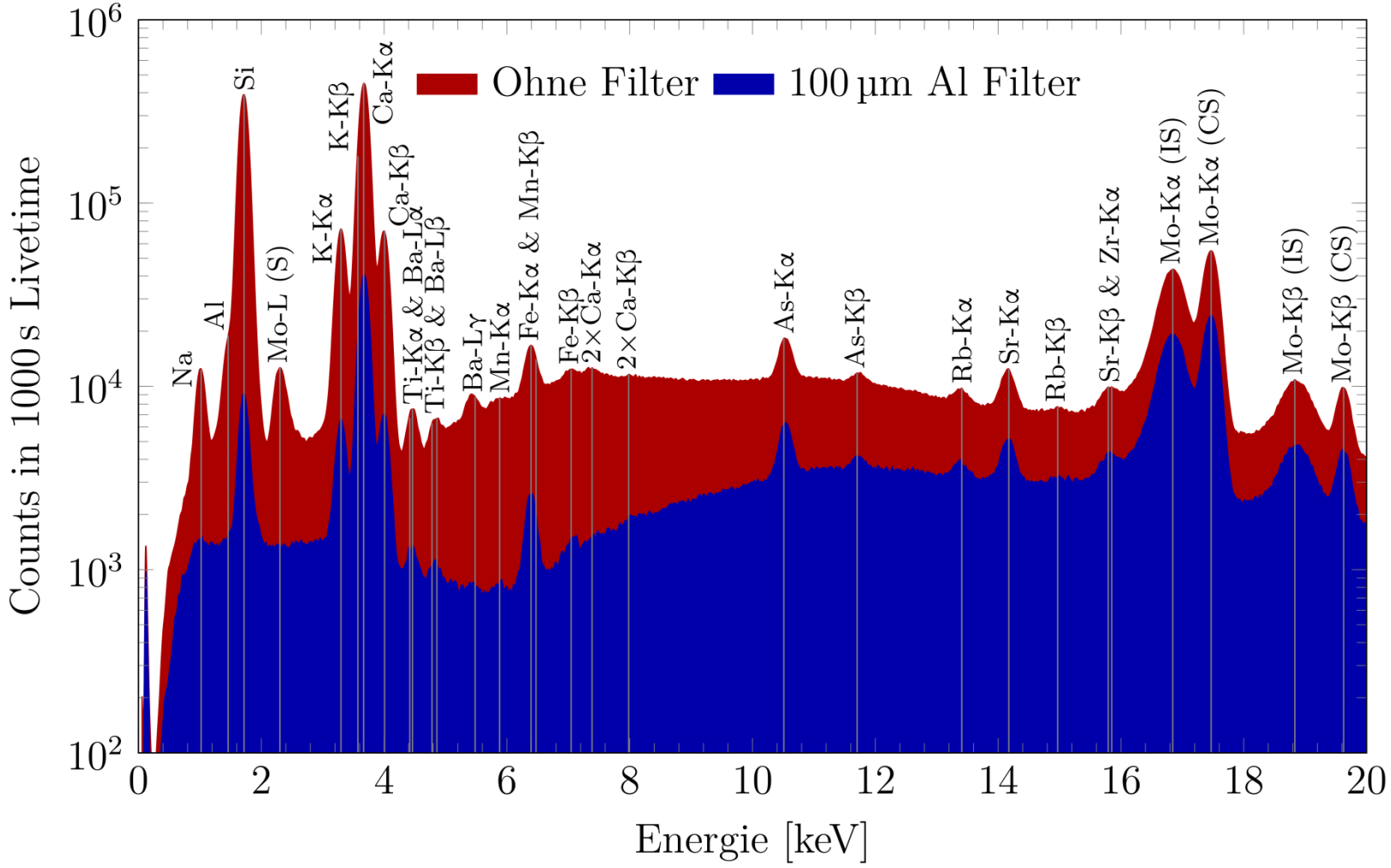

ATI µXRF Spectrometer

Determination of (LLD) using Standard Reference Material NIST621 Soda-Lime Container Glass:

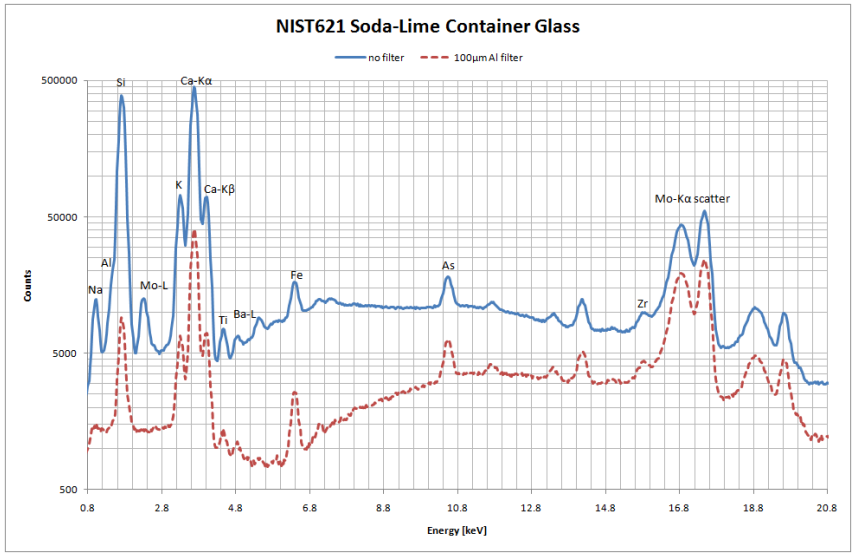

LLD

Element	LLD [ppm]	LLD (100µm Al filter) [ppm]
Na	878	36409
Al	115	4898
Si	95	2513
K	22	148
Ca	15	81
Ti	8	17
Fe	5	6
As	4	5
Zr	2	4
Ba	54	145

S. Smolek, C. Streli, N. Zoeger, P. Wobrauschek, Improved Micro-XRF Spectrometer for Light Element Analysis, REVIEW OF SCIENTIFIC INSTRUMENTS **81**, 053707 2010

Project supported by "Innovative Projekte" of TU Wien

$$LLD = m\frac{3\sqrt{N_B}}{N_N}$$

ATI µXRF Spectrometer future aspects

- confocale Extension of the Spectrometer
- Determination of the effective Spotsize (Volume) for different Elements
- Determination of the Transmission function of Polycapillaries
- Quantification models
- Measurement of various samples open projects (ANNA, …)

Confocal µXRF

- Measuring in a defined Micro volume
- 3D Analysis
- Information depth for thick samples solved as the actual depth is known

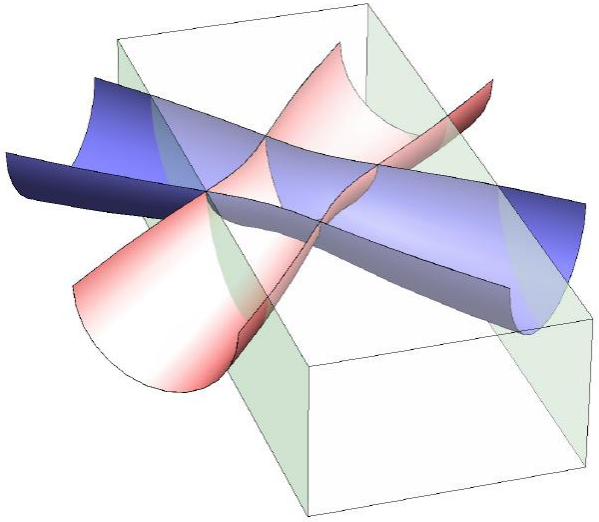

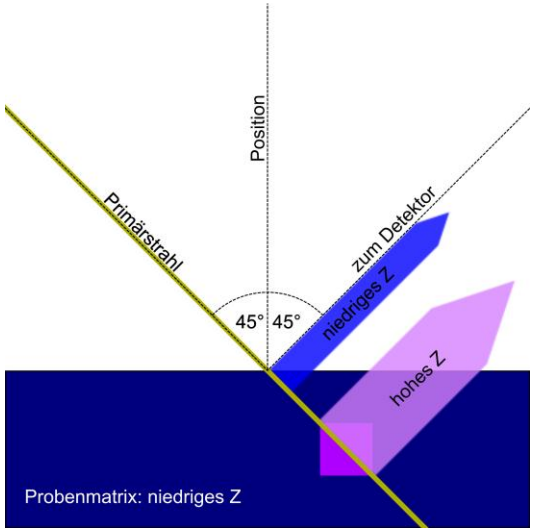

The Spectrometer

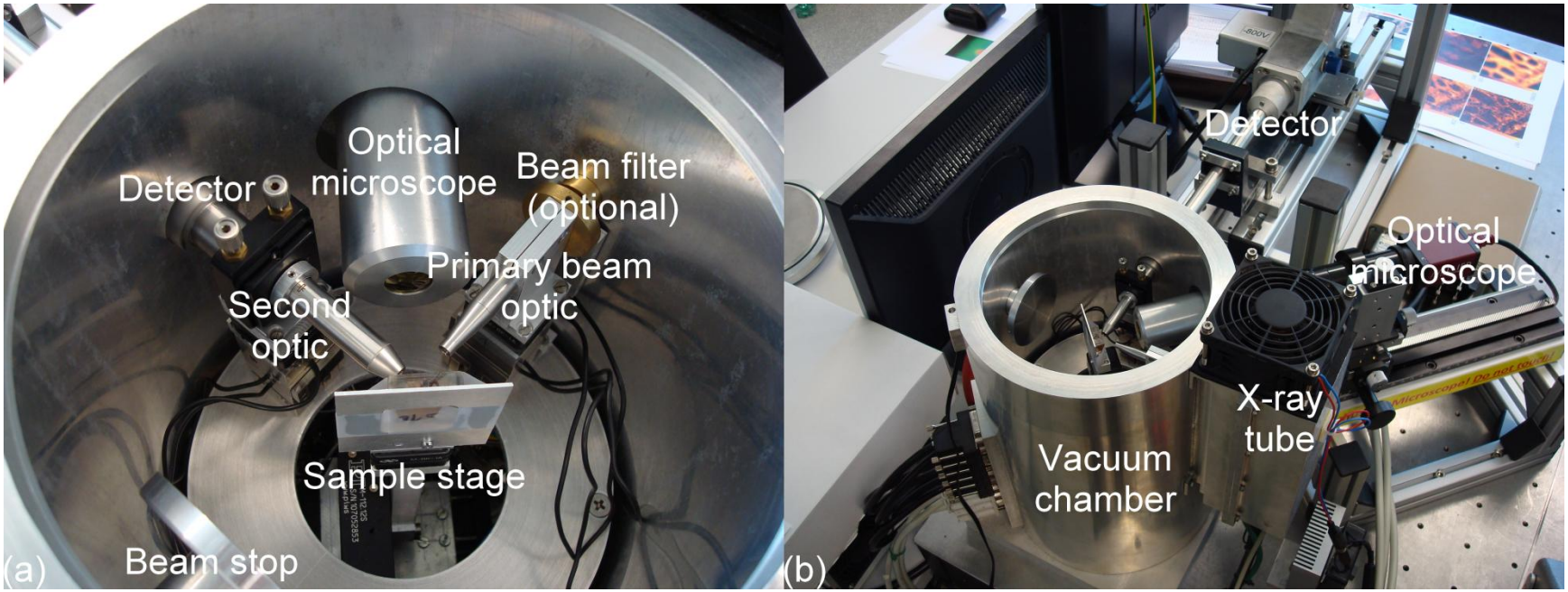

- **Improved micro x-ray fluorescence spectrometer for light element analysis.**
  Smolek S., Streli C., Zoeger N., Wobrauschek P.
  Rev Sci Instrum. 2010 May;81(5):053707.
- **Confocal micro-x-ray fluorescence spectrometer for light element analysis.**
  Smolek S., Pemmer B., Fölser M., Streli C., Wobrauschek P.
  Rev Sci Instrum. 2012 Aug;83(8):083703.

Components

- Air cooled low power microfocus X-ray tubes (Oxford "Apogee")
  - 35 µm spot size
  - 50 W Mo anode, 50 kV, 1 mA
  - 20 W Rh anode, 50 kV, 1 mA
  - Thin window (125 µm, Mo-L & Rh-L)
- Polycapillary X-ray optics (XOS)
  - Spot size: 32 µm @ Mo-Kα (17.44 keV)
- Optics x/y/z adjustment with attocube ANPx/z101 piezo positioners
  - 5 mm travel range

Control and measurement software

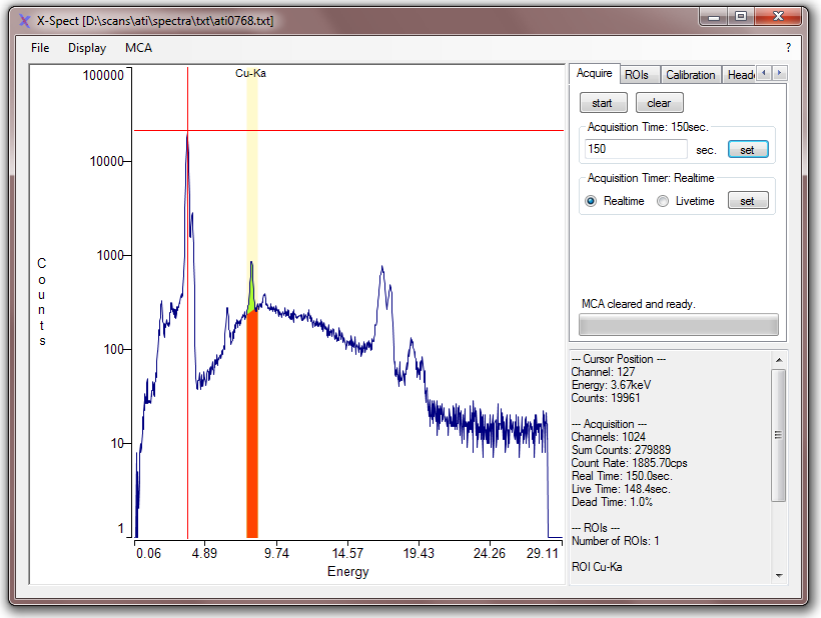

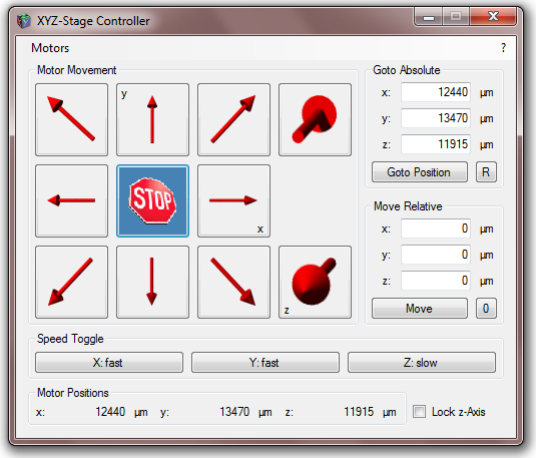

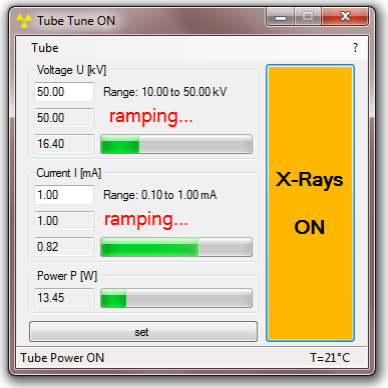

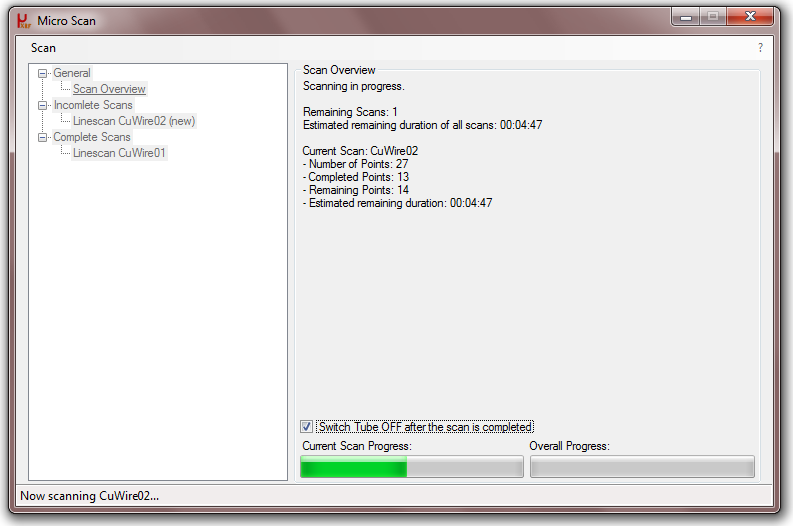

Confocal 3D analysis

- Scan parameters & data treat.:
  - 24x24x24 voxels
  - 10 µm steps
  - 5 s realtime acquisition
  - Mo X-ray tube at 50kV / 1mA
  - Gross ROI counts used
  - 3D data smoothed
- Red: 10µm Cu wire cross (Cu-Kα)
- Yellow: Gd x-ray screen (Gd-Lα)
- Blue: sticky tape (Mo-L scatter)

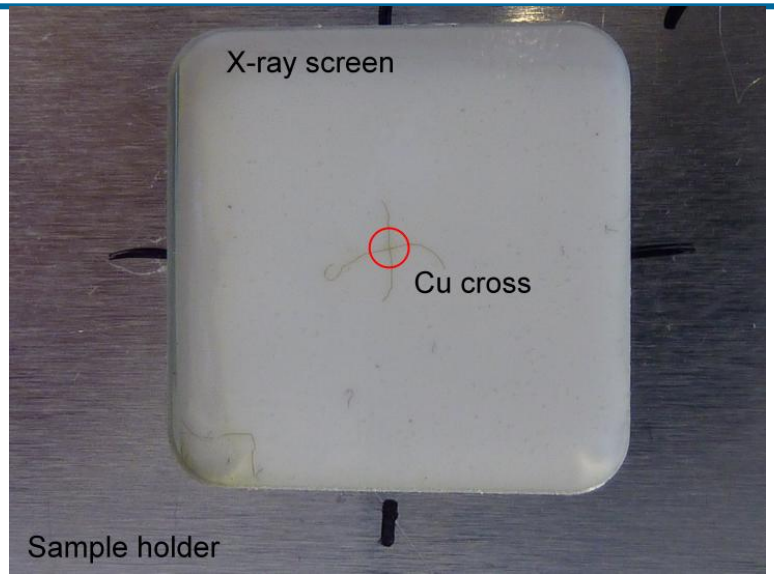

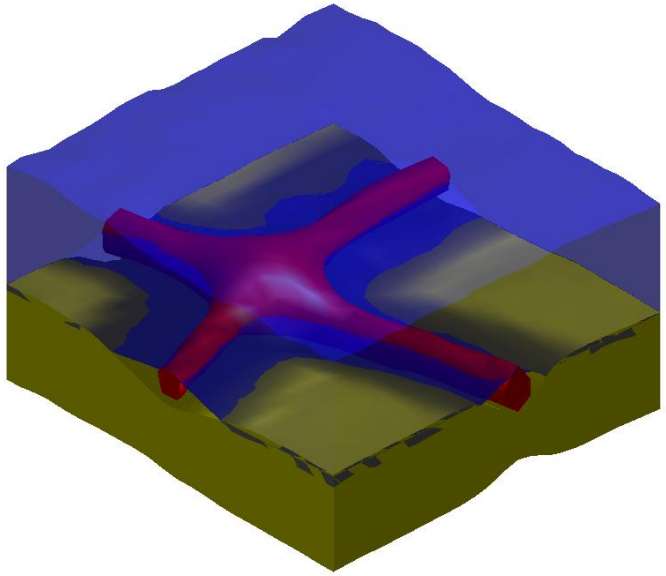

(Depth) resolution

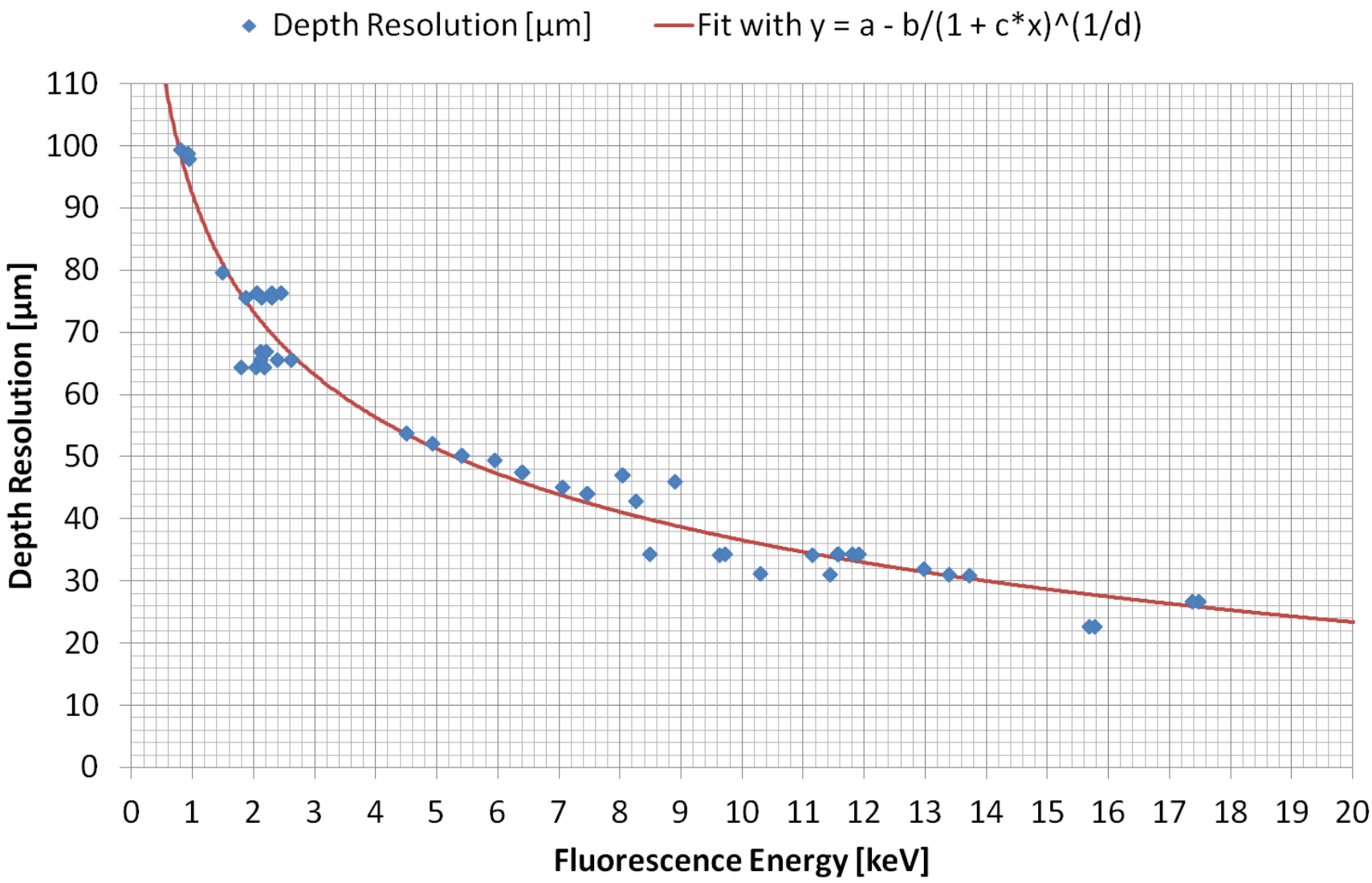

Depth profiling of paint layers

- Base: Cu
- Base coat: $PbCO_3.{}_2Pb(OH)_2$
- Metal overlay: Au
- Paint: HgS
- Paint: Fe_2O_3
- Paint: Pb_2SnO_4
- Paint: 2 $CuCO_3.Cu(OH)_2$

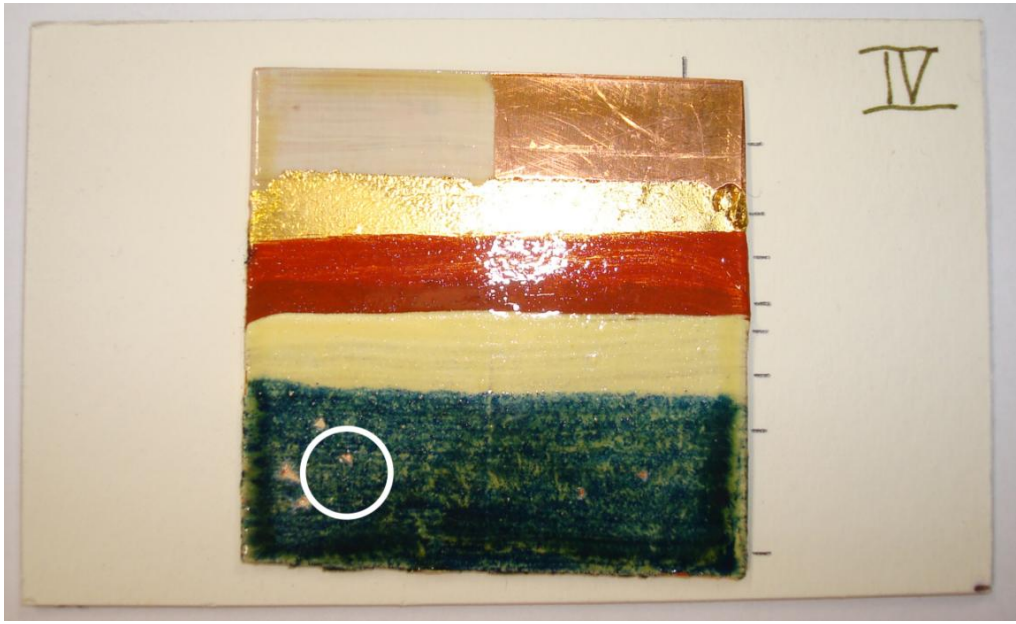

Depth profiling of paint layers

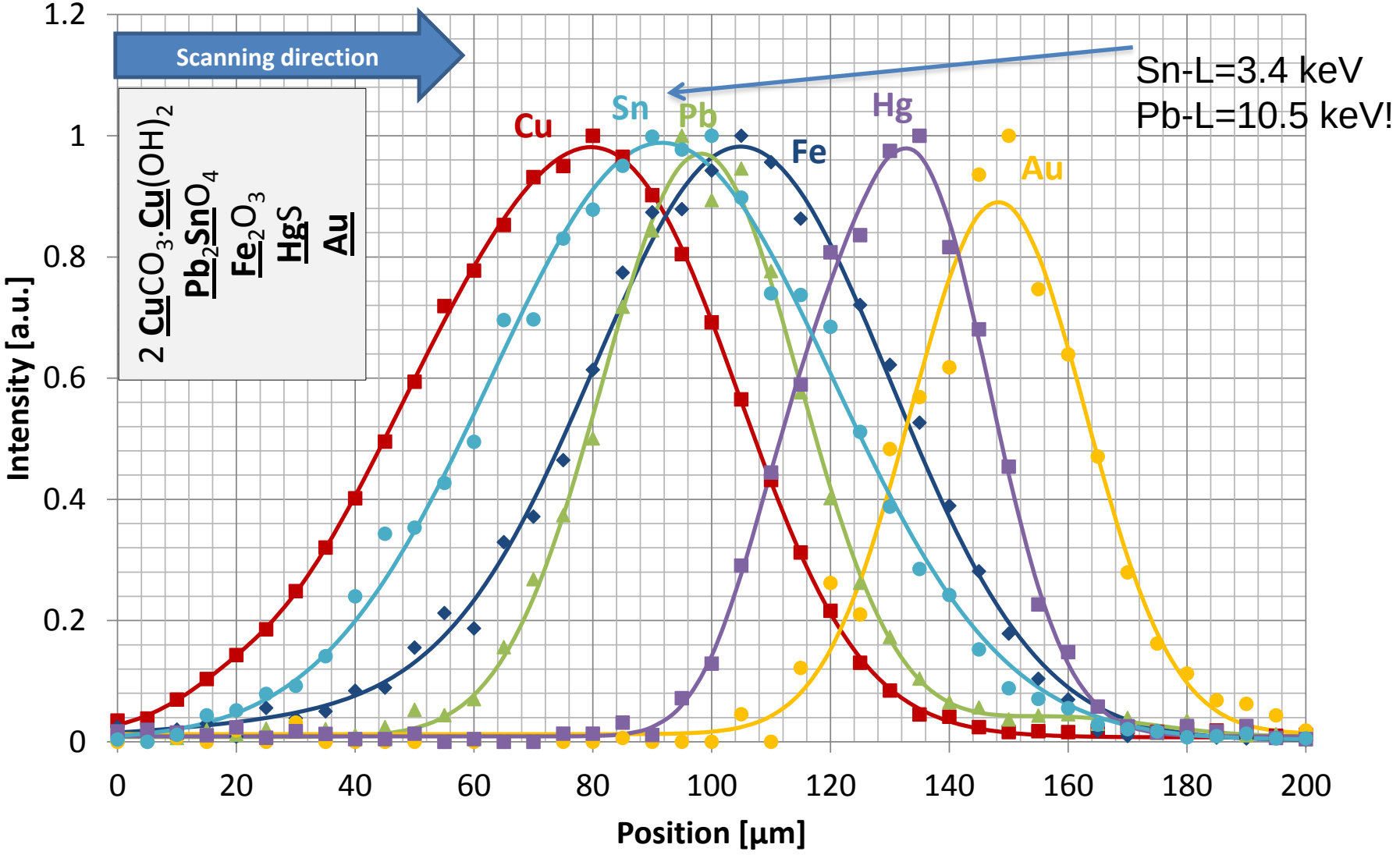

Bone Structure

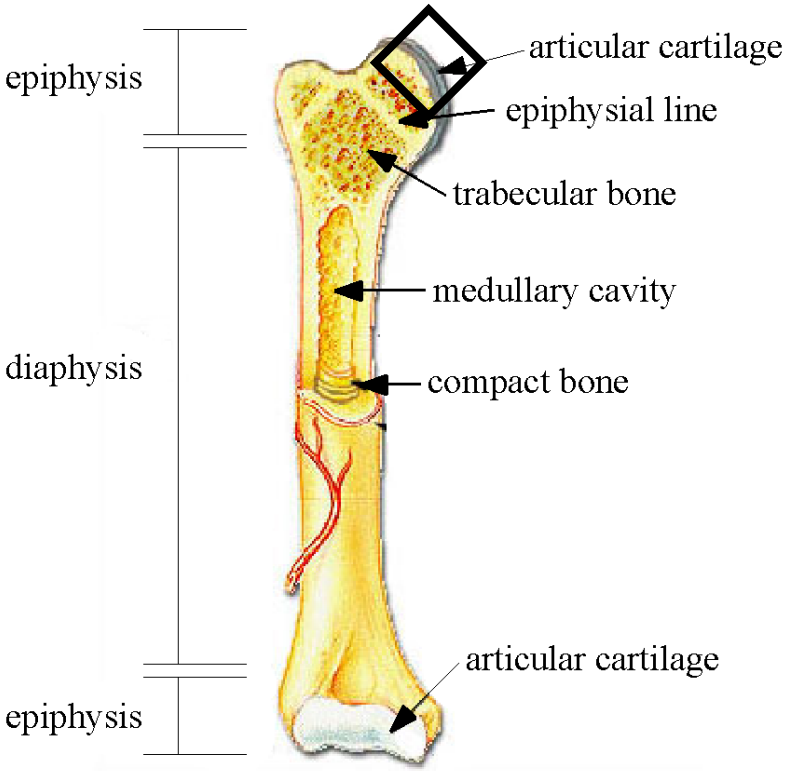

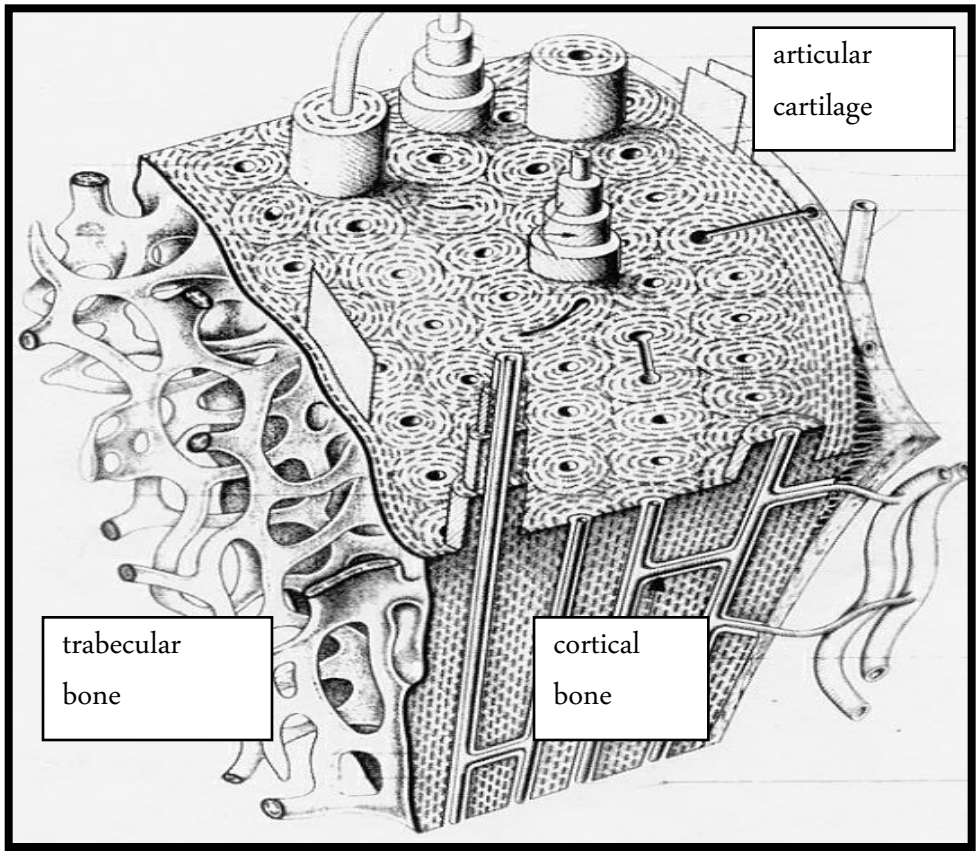

Patella - line scan

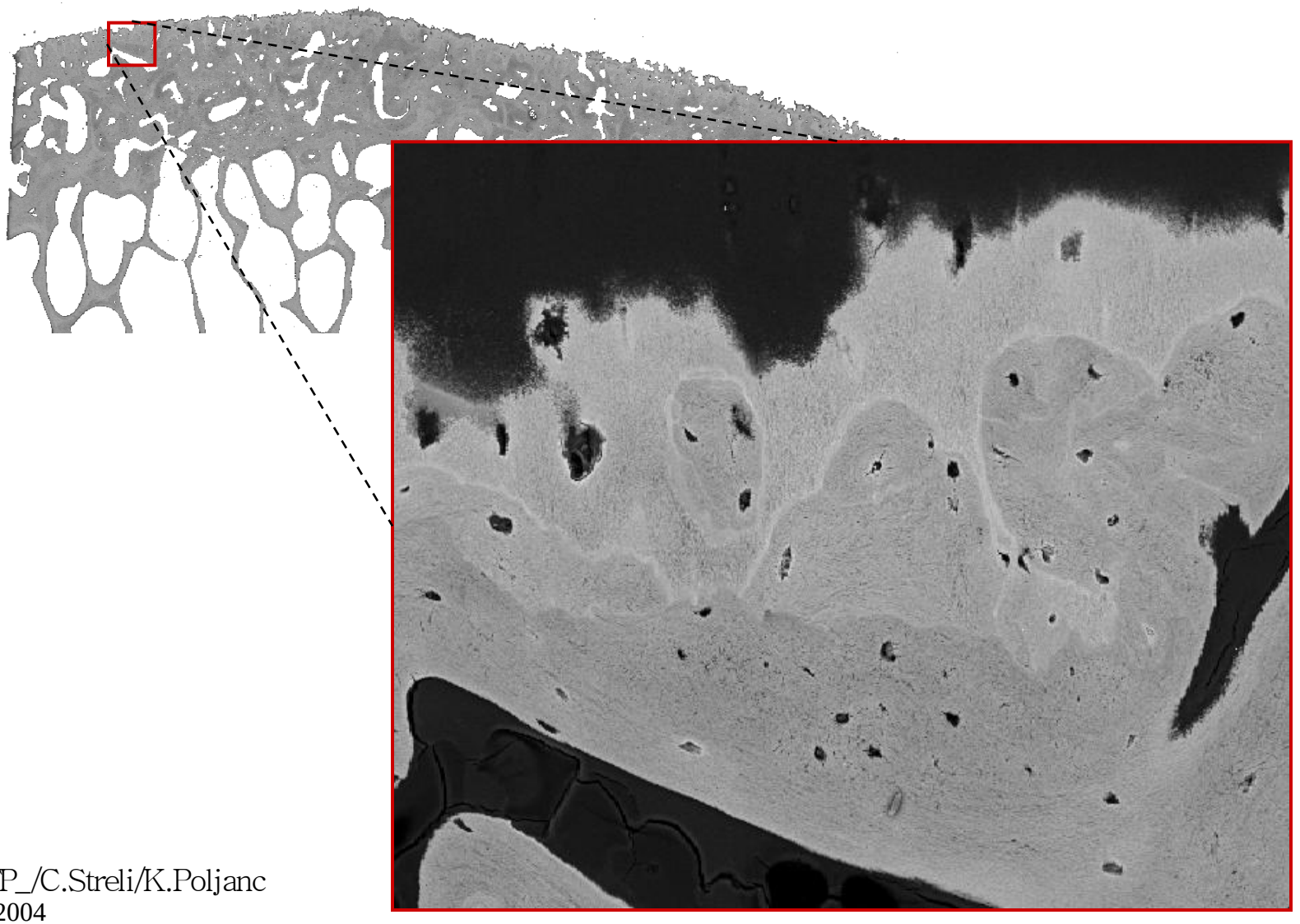

XRF-scans at HASYLAB-L

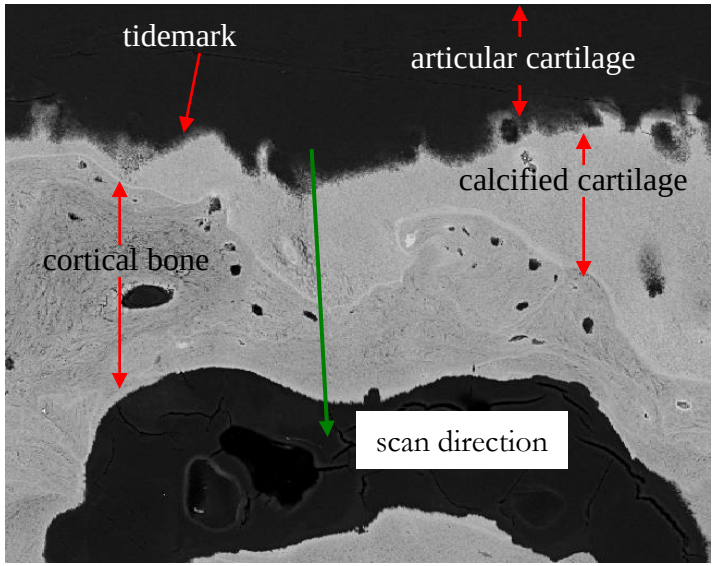

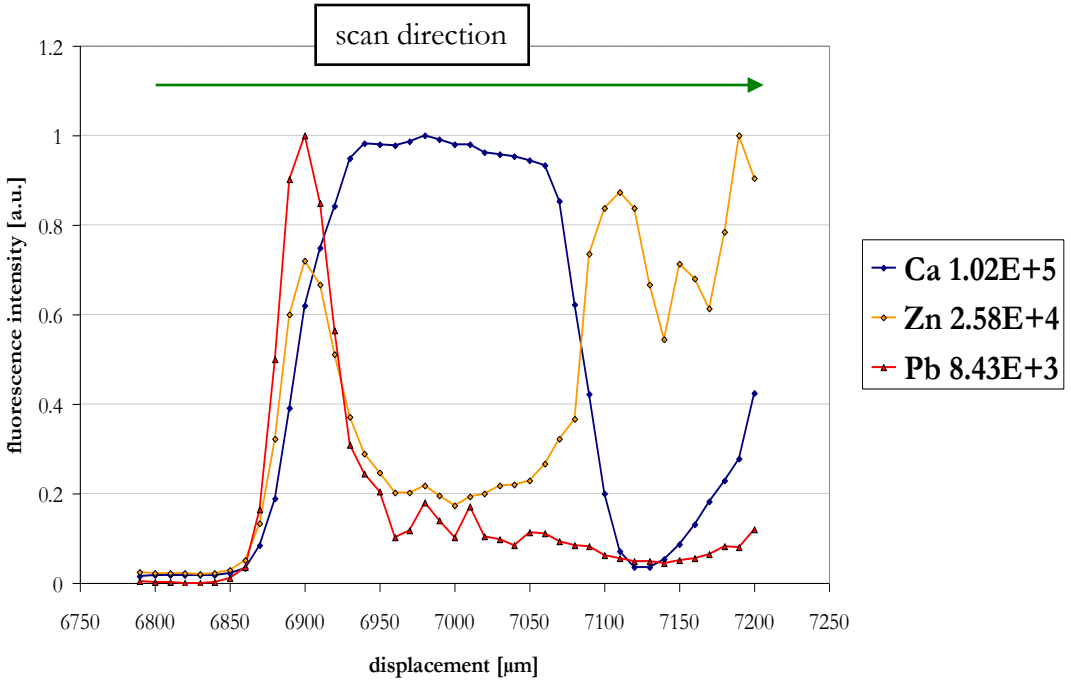

Interpretation: Sample Thickness Effect

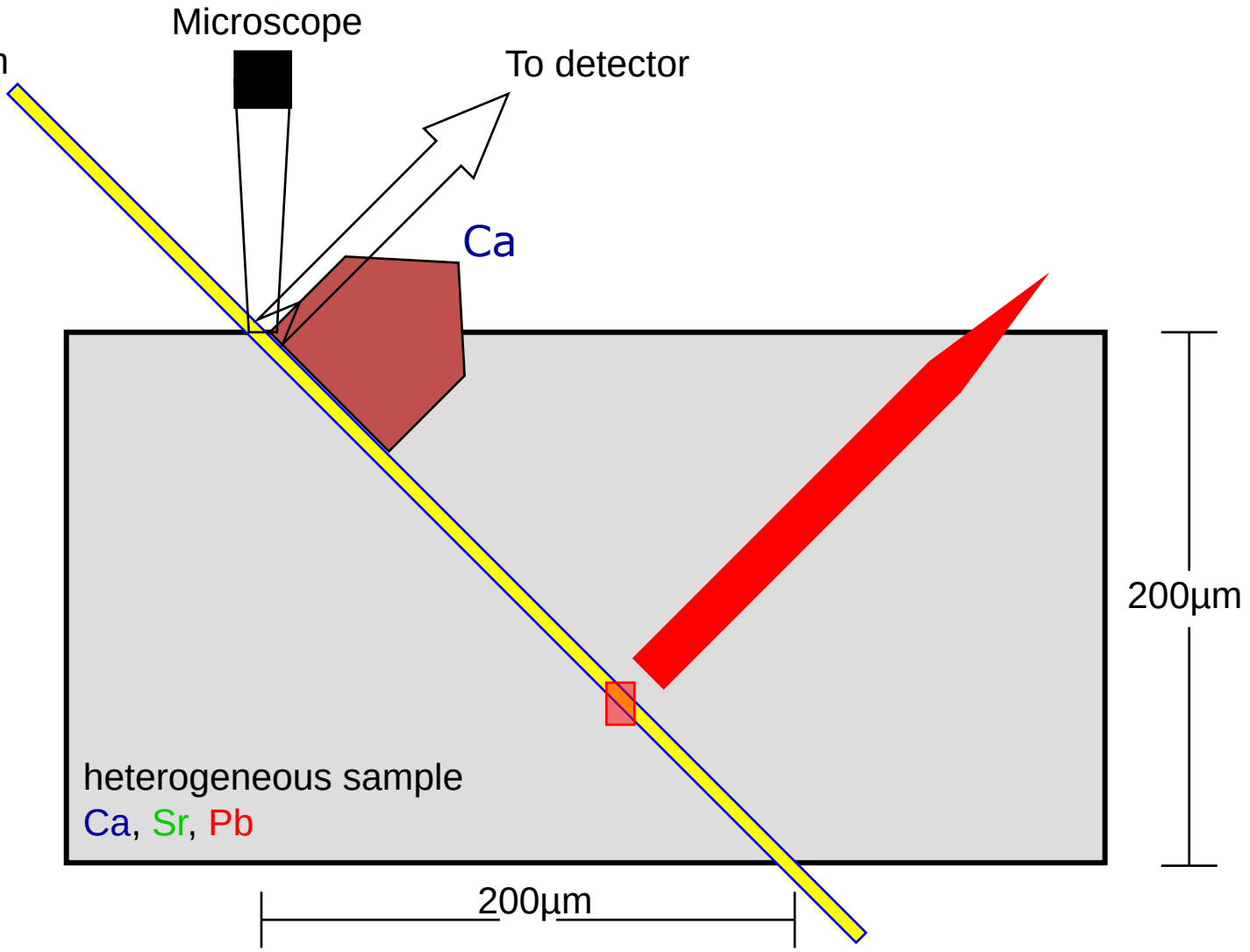

Information depth:
Ca ~ 40µm
Pb ~ 300µm
Sr ~ 600µm

Applet to show this effect

Setup at ANKA Fluo Beamline:

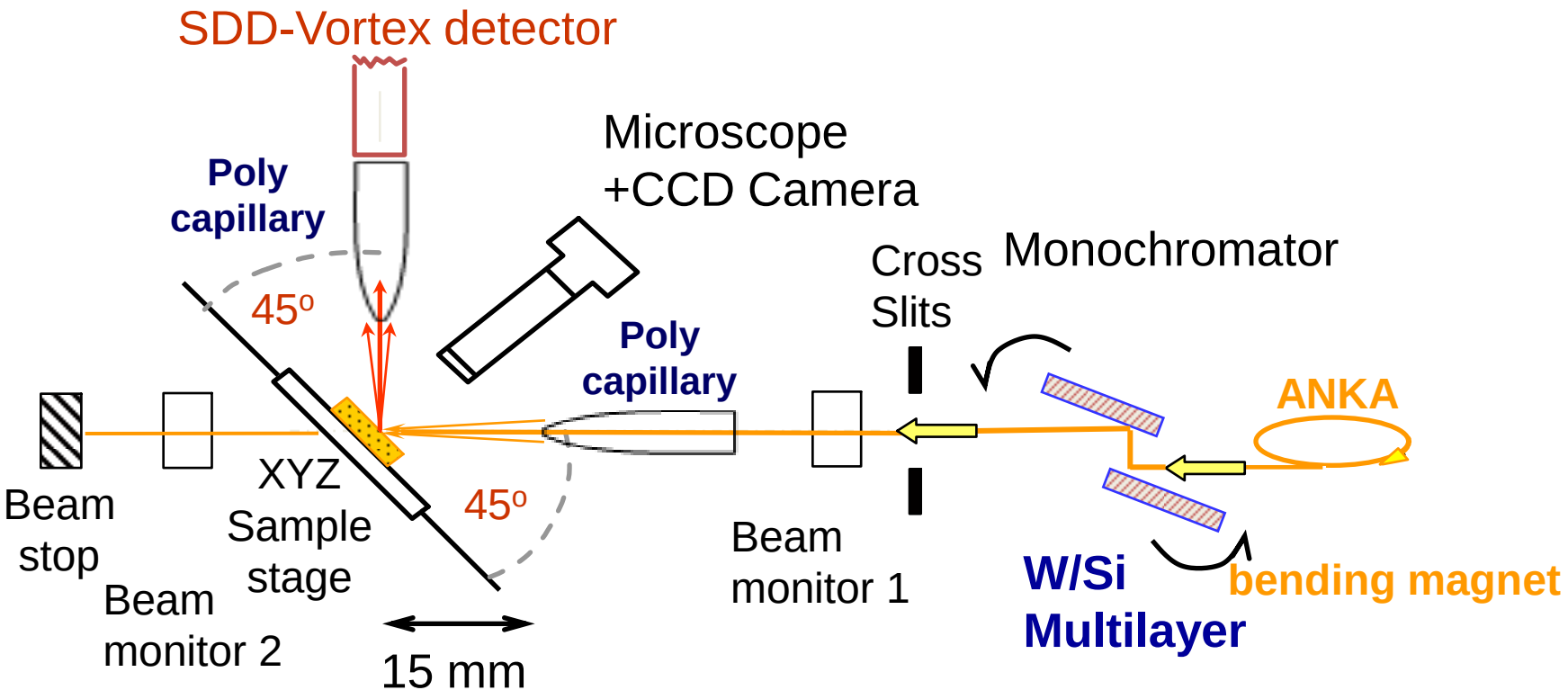

Focal size: ~10-20 µm
Depthresolution: ~15-20µm

Generation of the Elemental Maps:

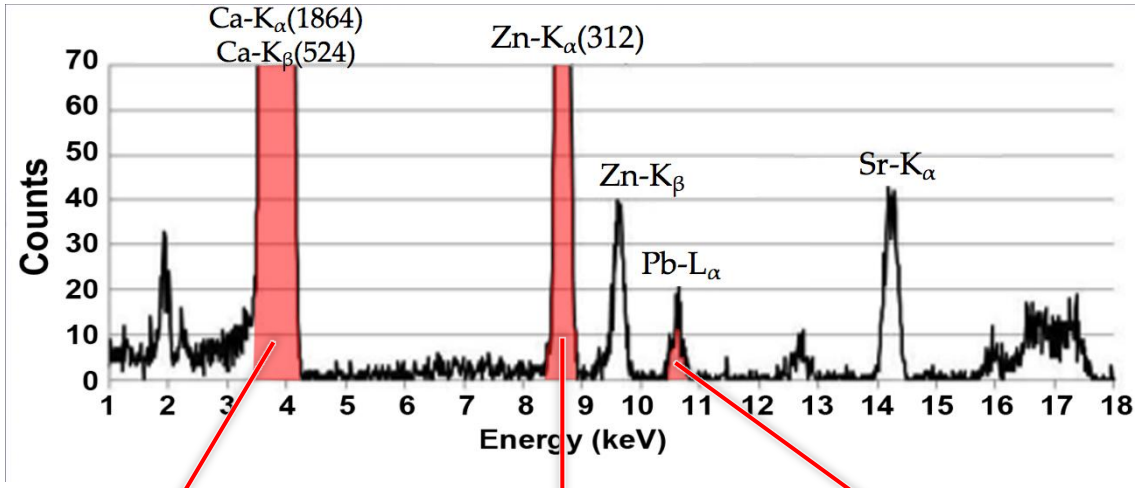

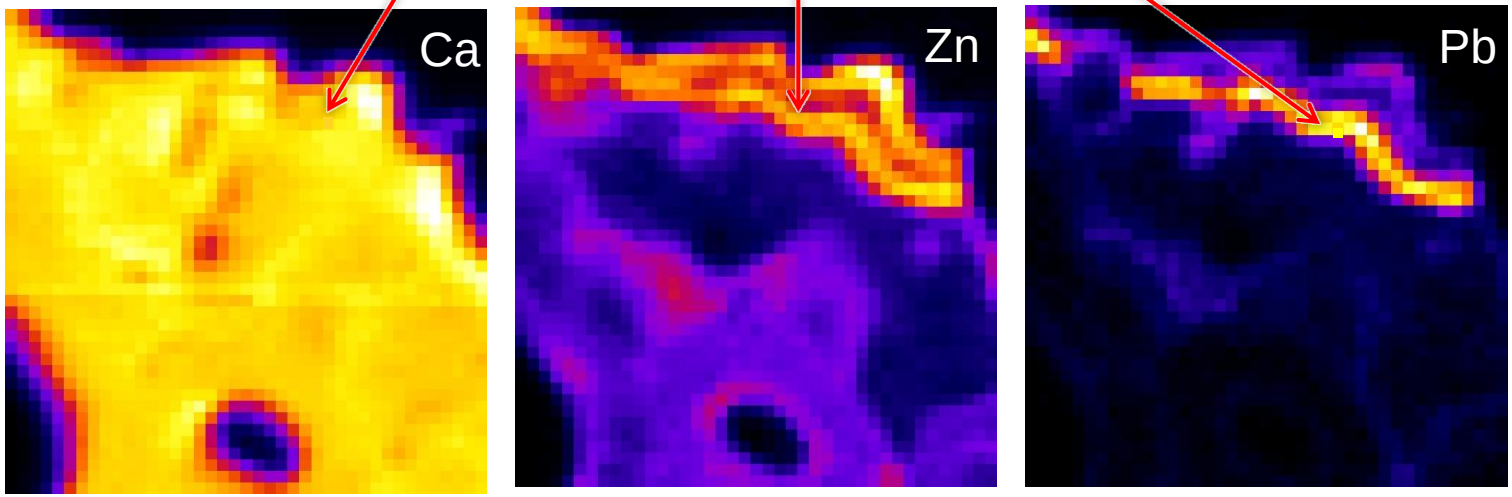

Portable ART analyzer (PART I & II)

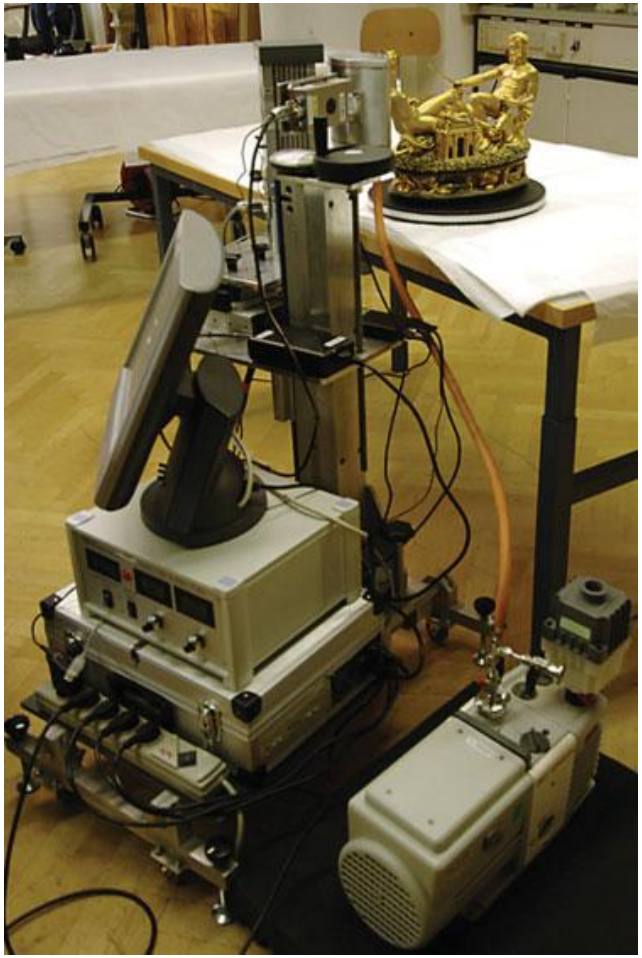

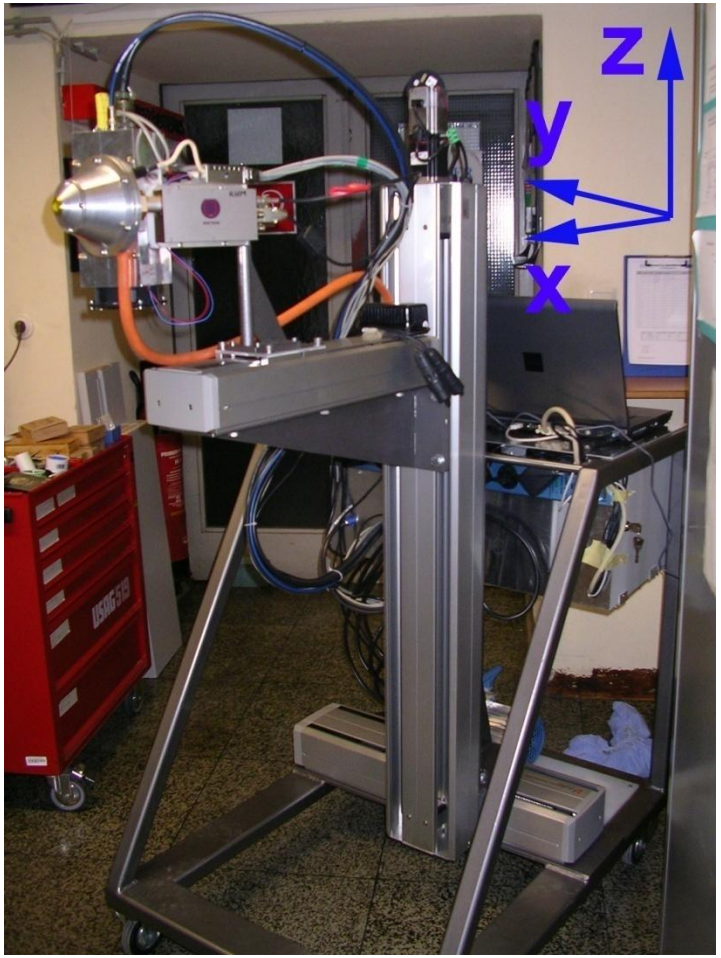

In cooperation with Art History Museum Wien and IAEA

PART II: Components

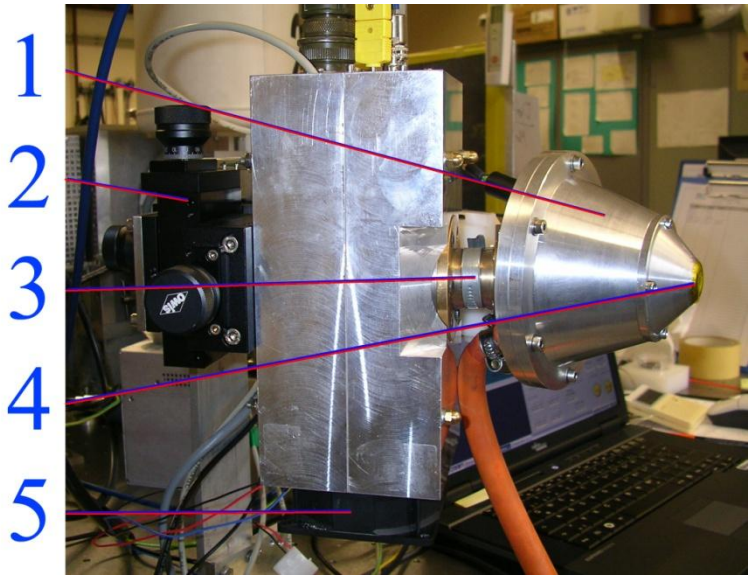

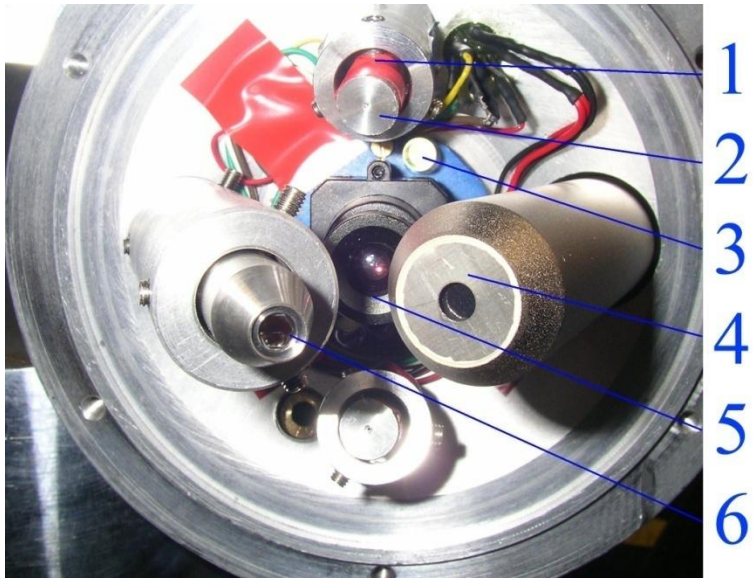

- Exchangeable x-ray tube (Mo /Cr) 50W
- Polycapillary x-ray optic (XOS), 145µm for Cr-Kα (5.41 keV)
- Ketek SDD, 20mm², 8µm Be
- Vacuumchamber

G. Buzanich, P. Wobrauschek, C. Streli, A. Markowicz, D. Wegrzynek, E. Chinea-Cano, M. Griesser and K. Uhlir, X-Ray Spectrom. 2009; 39: 98-102

PART I

Saliera B. Cellini 1540-43 produced

- 50kV/1mA Pd x-ray tube
- Polycapillary x-ray optic (160µm) or collimator (1mm)
- Ketek SDD, 10mm², 8µm Be
- Vacuum chamber

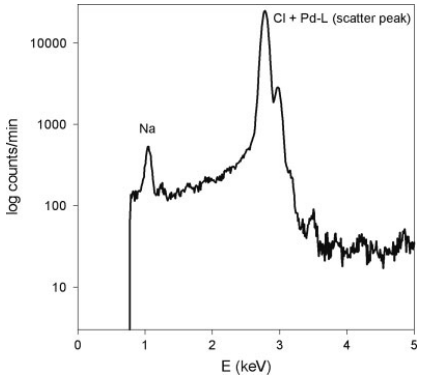

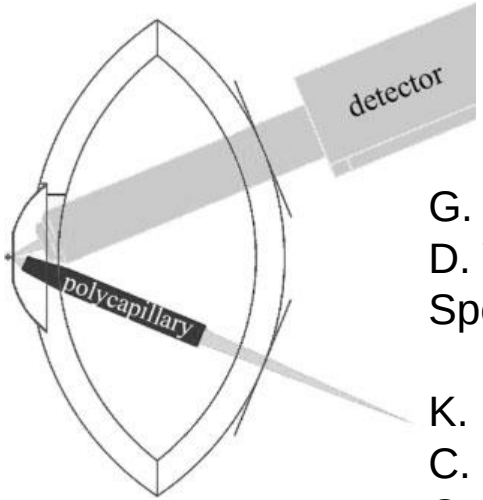

G. Buzanich, P. Wobrauschek, C. Streli, A. Markowicz, D. Wegrzynek, E. Chinea-Cano, S. Bamford, Spectrochimica Acta Part B 62 (2007) 1252 –1256

K. Uhlir, M. Griesser, G. Buzanich, P. Wobrauschek, C. Streli, D. Wegrzynek, A. Markowicz, E. Chinea-Cano, X-Ray Spectrom. 2008; 37: 450–457

PART I: Problems

- Too large shaped Vacuum chamber – not all interesting point on the object could be reached.
- Problems measuring paintings due to base holder of the chamber.
- Kapton™ window is bending towards inside and increases air gap, light elements as Na absorption in air.
- Laserspots were too large for 150 µm optic undefined position.

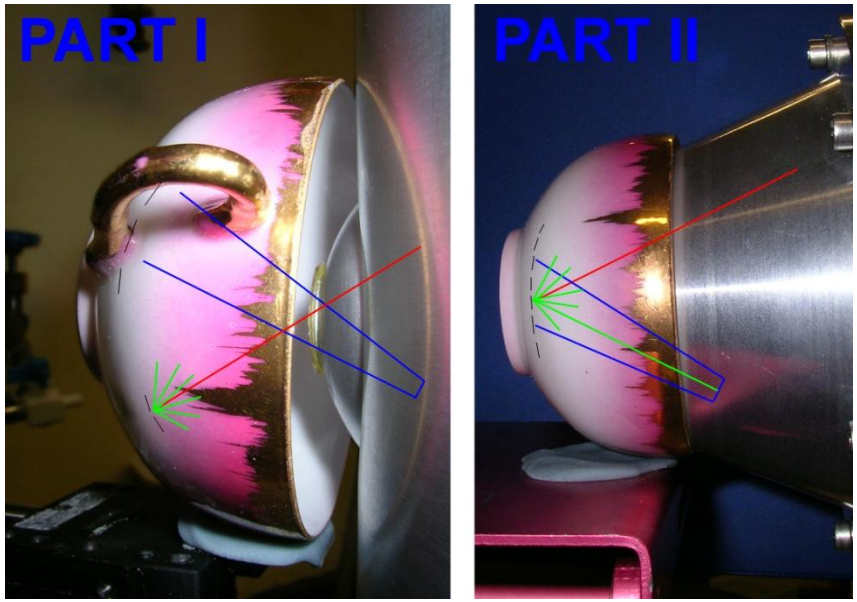

-> solution: New design PART II

PART II: Setup

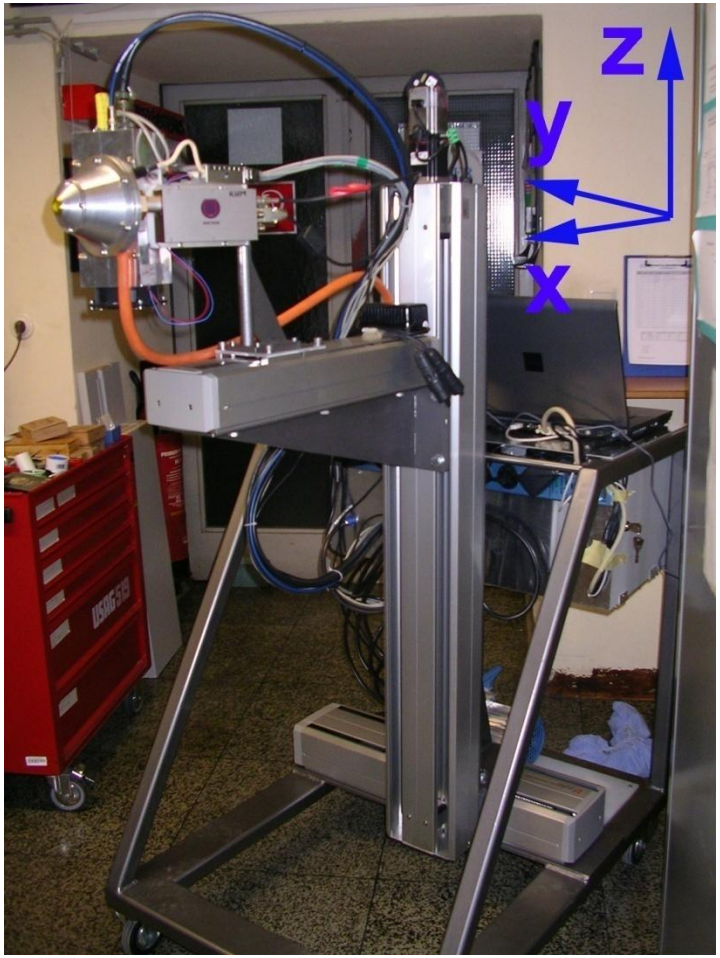

- Spectrometer motorized positioning (200 mm / 300 mm / 1000 mm depth x width x Height)
- Stable design of stand
- User friendly control

PART II: Tea cup

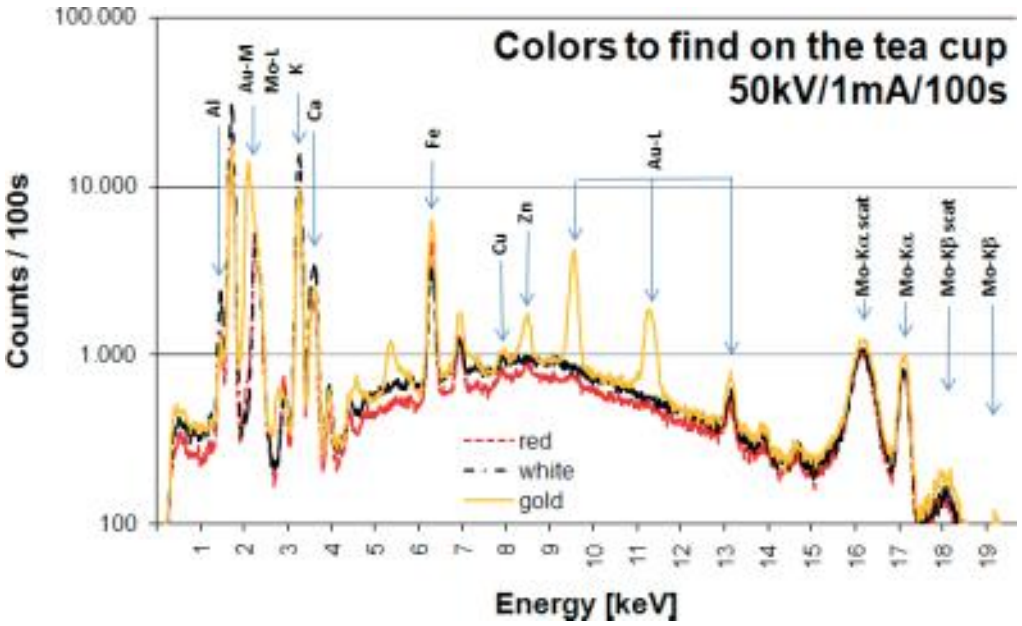

- Elemental composition of various colors of the tea cup:
  - Whíte: base material
  - Red: Higher Fe Gehalt, probably red Ockre. Small amounts of Zn point to a cup of the last century.
  - yellow: Gold

PART II: Detection limits LLD

Determination of detection limits (LLD) with NIST621 Soda-Lime Container Glass:

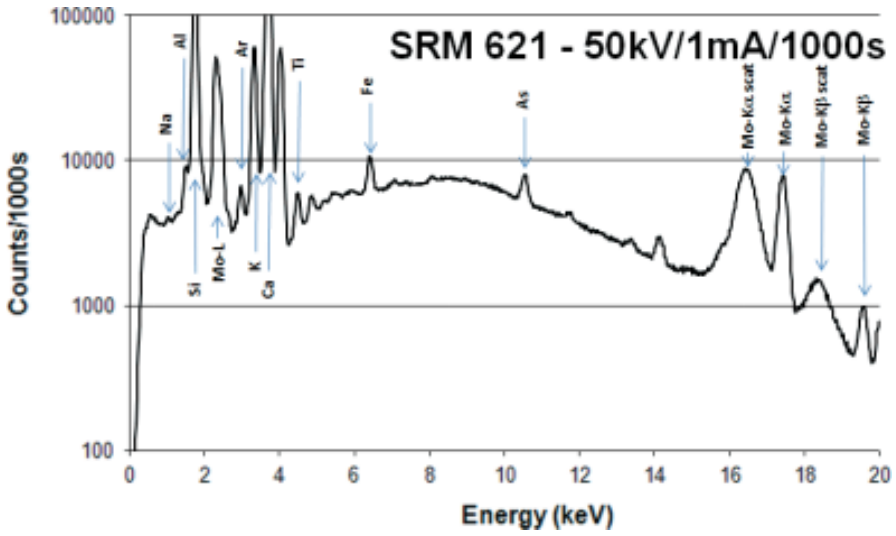

Element	LLD [ppm]
Na	7,69%
Al	452
Si	205
K	39
Ca	28
Ti	4
Fe	6
As	6

$$LLD = m\frac{3\sqrt{N_B}}{N_N}$$

Official radiation protection !!

THE END

THANKS FOR YOUR

ATTENTION